Superconductor Science and Technology

REVIEW

Multicomponent superconductivity based on multiband superconductors

To cite this article: Y Tanaka 2015 *Supercond. Sci. Technol.* **28** 034002

IOP Publishing Superconductor Science and Technology
Supercond. Sci. Technol. **28** (2015) 034002 (28pp) doi:10.1088/0953-2048/28/3/034002

Review

Multicomponent superconductivity based on multiband superconductors

Y Tanaka

National Institute of Advanced Industrial Science and Technology, AIST-Tsukuba-Central-2-3035918, 1-1-1 Umezono, Tsukuba, Ibaraki 305-8568, Japan

E-mail: y.tanaka@aist.go.jp

Received 25 July 2014, revised 8 September 2014
Accepted for publication 26 September 2014
Published 28 January 2015

Abstract

Multicomponent superconductivity is realized in multiband superconductors when an interband pairing interaction is considerably weaker than the intraband interactions. There is a new quantum phase that originates from the interband phase difference in this superconducting condensate. Firstly, we discuss the applicability of this physical viewpoint for known multiband superconductors. Secondly, topics related to the interband phase difference are treated. Finally, we mention that the Bardeen–Cooper–Schrieffer formalism and the Ginzburg–Landau formalism may not be fully guaranteed when we introduce a fluctuation in the interband phase difference mode. We also address plausible new superconducting electronics using the interband phase difference.

Keywords: soliton, fractional flux quanta, interband phase difference

(Some figures may appear in colour only in the online journal)

1. Introduction

The design and construction of the quantum phase are key issues in research regarding multicomponent quantum condensates. Realizing a new class of the quantum phase using multiband superconductors is a challenging endeavor. Searching for new phenomena and extracting new functions related to quantum phases had resulted in novel innovations such as the laser [1, 2] and superconducting quantum phase interference devices realized by the conventional system [3, 4]. Great innovations are required in implementing the quantum phase of the multiband superconductors such as the laser and SQUID. We survey current works and suggest a future study.

In this review, we illustrate the concept of multicomponent superconductivity based on multiband superconductors. It is considered that each band in a multiband superconductor has a condensate with an amplitude and phase that weakly interacts with the condensates of the other bands. The system has multiple quantum phases, which is not a straightforward extension of a conventional single-band superconductor with only one quantum phase; i.e., there is a leap in considerations.

Obtaining a suitable method for providing the multiple condensate to the multiband superconductor is a fundamental issue in science. Briefly, a strong intraband interaction and a weak interband interaction, that is, a contrast in the strengths of the interactions, is essential. A new gauge field appears when the system gains the multiple quantum phases. The functions and properties of these new gauge fields are yet to be understood. In these schema, the state of the system can be described by the Ginzburg–Landau formalism, with many connections to other ordered systems described in the same manner [5]. Multiple phases construct the internal phase outside of the three-dimensional space. The topologies have many common properties discussed in the field theory developed for particle physics [6–9], cosmological physics [10], and dissipative classical systems having a complex vector field [11–16].

These new quantum phases are also attractive for the fabrication of novel electronic devices [17]. The properties of the new gauge field are completely different from those of the

conventional superconductor. Some components of the gauge field are electromagnetically inactive and cannot be accessed using the conventional electro-magnetic field [18–23]. There have been some proposals regarding how to control it [22, 24, 25]. In one such technique, an ingenious new device is disconnected from the environment completely. One application of this electromagnetically inactive device is a quantum Turing machine in which the decoherence time becomes infinitesimally prolonged in an ideal situation because of the complete decoupling from the electromagnetic field existing in the environment [17].

Several materials are candidates to realize the multicomponent superconductivity based on multiband superconductors. Historically, the transition metals, such as Nb and V, were considered to have a multiband nature [26, 27]. A Leggett mode, which is a small interband phase difference fluctuation (with coupling to the amplitude modes) was theoretically discovered for these materials [28]. $NbSe_2$ [29], graphite intercalation compounds [30, 31], and the Chevrel compound [32] were investigated similarly. Multilayer cuprate superconductors such as $CuBa_2Ca_3Cu_4O_y$ (Cu-1234), which is obtained by substituting Ca-CuO_2-Ca for the Y in YBa_2Cu_3Oy (Y-123) and has four CuO_2 planes in one unit cell, exhibits the multiband nature [33, 34]. It was experimentally suggested that the interband interaction is two orders of magnitude smaller than the intraband interaction [35, 36]. Cu-1234 is the first material satisfying the Leggett condition, whereby the interband interaction is far smaller than the intraband interaction. Consideration of the basic properties of this material suggests the interband phase difference soliton (*i*-soliton), in which the interband phase difference rotates by 2π radians [20, 21]. Indeed, there is an experimental indication of the formation of the vortex molecule composed of the fractional vortex and interband phase soliton in $CuBa_2Ca_2Cu_3O_y$ (Cu-1223), which is a member of the family of Cu-1234 [37–39]. Now, MgB_2 [40] and pnictides [41] are also considered as attractive candidates. The artificial structure, such as a thin $Al/AlO_x/Al$ multilayer, is the most promising platform for the study of the *i*-soliton [42]. When the multilayer is far thinner than the magnetic penetration depth, it is considered to mimic the multiband superconductor. The direct observation of the *i*-soliton [42] and fractional vortices [43, 44], which constitute symbolic topology discussed in the multicomponent superconductivity, were reported using the multilayer system.

This review is organized as follows. Section 2 briefly discusses the history of the multiband superconductor leading the multicomponent superconductivity. Section 3 introduces topics related to multicomponent superconductivity based on multiband superconductors. The following topics are introduced: the Leggett mode, i.e., a small fluctuation in the interband phase difference [28]; the interband phase difference soliton, i.e., a soliton in which the interband phase difference rotates by 2π radians [20, 21]; the fractionalization of the flux quanta and fractional vortex—when the *i*-soliton is attached a hole (the hole at the center of the doughnut, not a hole of the quasi-particle) or vortex, the boundary condition generates the fractional flux quanta (non-integer multiple of the unit flux quantum, Φ_0) [21, 45]; a massless mode, i.e., a soft mode of the Leggett mode [46–48]; and the interband phase difference frustration, whereby a competition among several interband interactions invokes the non-trivial phase difference, which is neither π nor 0 radians [20, 49–51]. The effect of the entropy of a Bardeen–Cooper–Schrieffer pair (BCS pair) is also introduced [52]. The three topics—the massless mode, frustration, and entropy of the pair—closely relate to each other and are introduced in the same section. The superconductivity that is neither type I nor type II, as evident from the multicomponent nature (type 1.5 superconductivity) [53, 54], is also closely related to the problem of the entropy of the pair. This subject is also discussed in the section 3.1. The non-superconducting multiple components and multi-order-parameter systems, such as an atomic gas Bose–Einstein condensate [55, 56] and superfluid ^{3}He [57–59], are examined for a comparison to multicomponent superconductivity.

2. An historical survey

2.1. From the BCS theory to the multicomponent superconductivity based on multiband superconductors

The original microscopic theory of the superconductivity by BCS theory was a simplified model for an isotropic single superconducting gap, which is suitable for basic properties such as the excitation spectrum and the emergence of superconductivity due to an evolution of the superconducting gap of superconductors that were known at that time [60]. The model has considerable room for refinement, e.g., introducing multiple superconducting gaps. Suhl, Matthias, and Walker proposed two-band extension in 1959, two years after the BCS theory was proposed [61]. The motivation of this work was to explain the relatively high transition temperature (T_c) observed for transition metal superconductors [27]. Two different magnitudes are assigned to two different superconducting gaps, whereas the superconducting phase is identical for the two gaps. In 1962, Kondo [62] and Peretti [63] independently introduced different phases for different gaps due to the non-electron phonon-mediated superconductivity speculated to exist owing to the vanishing of the isotope effect in some transition metal superconductors, such as Ru and Os. The phase difference between two gaps is π radians, indicating sign reversal gaps. Leggett introduced a phase difference other than 0 or π radians as a collective excitation potentially present in the transition metal superconductors [28]. This is a small fluctuation in the phase difference now called a 'Leggett mode.' In 2001, Tanaka extended this fluctuation to 2π radians [20, 21], yielding an interband phase-difference soliton (*i*-soliton). The very weak interband interaction discovered in the multi-layer cuprate superconductor Cu-1234 in 1999 [35, 36] was a trigger for this finding. This work considered the topology and multiple components with regard to the superconductivity in the multiband superconductor. Once a multicomponent picture was introduced for the multiband superconductor, the physics involving a field theory admitting multiple gauge fields could be examined [18, 23, 64–69]. The physics of MgB_2 and pnictides has been frequently discussed according to this picture since 2001 [70].

Herein, to explicitly specify a superconductor having multiple components according to the multi-band electronic structure, we use the term 'multicomponent superconductivity based on multiband superconductors.'

A picture of the multicomponent superconductivity based on multiband superconductors has not been constructed straightforwardly since Suhl, Matthias, and Walker reported their calculation [61]. Sometimes, there were leaps in the logic. These leaps are reflected by the usage of terms such as 'anisotropic gap,' 'multigap,' 'multiband,' and 'multicomponent.' We discuss these terms in the next section. Then, we describe the consequences of the multicomponent nature which was or would be observed in the multicomponent superconductivity based on the multiband superconductors.

2.2. Multiband superconductors and multigap superconductors

The terms 'multiband superconductor' and 'multigap superconductor' do not always indicate the same meaning and physics, which seem to vary by researchers and subjects. Such physics terminology is summarized in this section.

Important issues include the deviation from an isotropic single gap and how this can be modified. All real superconductors have the ability to change the isotropic magnitude, phase, and temperature evolution of the gap.

The first step of the modification is introducing the effects of the anisotropy of the Fermi surface [71] and pairing interaction [72], which modify the magnitude of the gap. In these works, it was demonstrated that the gap varies continuously on the Fermi surface. Here, the Fermi surface is that of the normal state. The temperature dependence of the magnitude of the gap normalized by that at 0 K is in principle identical to that of the isotropic single gap [71]. Gross, Massidda, and their collaborators are constructing an ultimate modern version of the *ab initio* calculation of the anisotropic gap [73].

The second step is introducing two discrete magnitudes into the gaps, as Suhl, Matthias, and Walker did [61]. Two gaps originate from two bands. There are three points that should be noted here. The first is that the magnitude of the gap on one band is different from that on another band. The second is that the superconductivity can emerge by the interband interaction only without the intraband interaction. In this case, the temperature dependence of the magnitude of the gap normalized by that at 0 K for each band is similar to that of the isotropic single-gap case. That is, it behaves as a single-component superconductivity, even though there are two gaps. Thirdly, the temperature dependence of the gap normalized by that at 0 K differs considerably from that of the isotropic single-gap case when the interband interaction is far smaller than the intraband interaction. That is, it behaves as a double-component superconductivity. We note that the cases denoted by the third and second points should be crucially distinguished considering the collective excitation. The interband phase difference fluctuation can be a good picture for the collective excitation for the third case, whereas the mixing of the anisotropic gap with the nodes in one band can also be a collective excitation having the same energy scale as the interband phase difference fluctuation in the second case.

In Suhl, Matthias, and Walker's work, the condition of the multiband is converted into the pair interaction and density of the state. Within the same band, the magnitude of the intraband pair interaction is the same, as is the density of the state. There is a difference in the magnitude of the intraband interaction and the density of the state between two bands. The magnitude of the interband interaction is also the same throughout the Fermi surface. These conditions are natural assumptions for a system having multiple electronic bands but are neither absolute nor inevitable consequences of using multiband superconductors. For example, we can assume the situation in which a system has one band but can be divided into two sectors having an individual intra-sector interaction. On the contrary, even when the magnitude of the intraband interaction of one band is equal to that of another band and we never see 'two gaps' in the tunneling spectrum and specific heat, the weak interband interaction may cause apparent properties such as an interband phase difference fluctuation. The essential issue is the contrast in the strength of the pair interaction rather than the band structure itself. Suhl, Matthias, and Walker did not discuss the sole case. They discussed two cases: one exhibited a contrast in the strength between two intraband interactions or in the density of the state between two bands, causing two gaps, and the other exhibited a contrast in the strength between the intraband interaction and interband interaction, causing two components when the interband interaction was very weak. Each band could have any phase and magnitude of the gap. This is the multicomponent superconductivity based on multiband superconductors.

Since the 1960s, seeking the anisotropic gap and multiple gaps has been a major focus in the study of the multiband superconductor. Shen, Senozan, and Phillips (UCB) reported that there are two exponential terms in the heat capacity of a pure Niobium sample [26]. They concluded that this reflects the two gaps discussed by Suhl, Matthias, and Walker. In 2001, Phillips's group (UCB) applied this method to MgB_2 and identified two gaps in the heat capacity [74, 75]. More recently, Nakajima *et al* applied the method to ternary-iron silicide, $Lu_2Fe_3Si_5$ [76]. The technique can be considered as the identification of the multiple gaps (not multiple components). The model of the anisotropic gap can also improve the fitting of the experimental data compared with the fitting using the single isotropic gap model [77–79]. For the thermodynamic properties, the effect of the anisotropy of a gap can be reproduced by several gaps having different discrete values. The effect from the several gaps can be also reproduced by the anisotropic gap. When the temperature dependence of the magnitude of a gap normalized by that at 0 K can be reproduced by that of a single isotropic gap, the fitting by an anisotropic gap and multiple gaps tend to yield similar results. Some theoreticians utilize the results of *ab initio* calculations to judge whether the superconducting gap is continuously distributed (anisotropic superconductor) or not (multigap superconductor) [73, 80–83].

Table 1. Crude classification of superconductivity on multiband superconductors by strength contrast in a pairing interaction. This is the simplest classification. Situations describing real materials occur between these classifications.

The first band	The second band	The interband	Superconductivity
Strong	Strong	Weak	Two-component
Strong	Weak	Strong	Two-gap, single-component
Strong	Weak	Weak	Two-gap, single-component[a]
Strong	Strong	Strong	Single-gap[b], single-component
Weak	Weak	Strong	Single-gap[b], single-component

[a] There may be a small correction needed to reproduce the experimental data absolutely.
[b] They may be two-gap when there is a noticeable difference between two intraband interactions.

In a more advanced procedure, the difference in the temperature dependence between the magnitudes of the two gaps is considered [84]. As Suhl, Matthias, and Walker mentioned, if an interband interaction is weak [61], the gap evolution is not reproduced by a single isotropic gap model. The gap evolution being different from that of the single anisotropic gap becomes a key issue. Tokunaga *et al* (Osaka Univ.) and Ihara group (AIST) found the first example of this by applying the ^{63}Cu nuclear magnetic resonance (NMR) technique to the multilayer cuprate superconductor Cu-1234 [33] in 1999 [35]. Cu-1234 has at least two superconducting components because it has four superconducting CuO_2 planes in one unit cell, causing multiple bands [34]. Using the Knight shift, they evaluated the gap evolution on one component, which is strictly different from that of an isotropic single gap. This tendency was confirmed by a specific heat study by the same group [36]. There was a broad peak around 80 K in addition to a jump due to the superconducting transition at 117 K. They analyzed the heat capacity data using a two-gap model accounting for the weak interband interaction reproducing the anomalous temperature dependence as demonstrated by Suhl, Matthias, and Walker. This weak interband interaction was not considered in [26, 74, 75]. The very weak interband interaction (on the order of a few percent of the maximum strength of the intraband interaction) can reproduce the second broad peak in the heat capacity, but the moderately weak interband interaction (on the order of ten percent of the maximum strength of intraband interaction) does not reproduce it. These anomalous thermodynamic properties and gap evolutions were revisited theoretically by Vargunin, T Örd, and K Rägo in 2011 [85] and 2013 [86]. The abnormal gap evolution in a two-component superconductivity based on multiband superconductors was experimentally reported as an abnormal temperature dependence of the superfluid density estimated by the penetration depth using the muon-spin rotation (μSR) technique for $FeSe_{1-x}$ [87].

There are five cases regarding the strength-contrast in pairing interactions, as summarized in table 1. The first is the case of two strong intraband interactions and a weak interband interaction. This is an ideal situation for the emergence of a two-component superconductivity. Two different magnitudes for the gaps is not essential for the two-component superconductivity, as described before. When one intraband interaction is so weak, we can observe the signatures of the two gaps using experimental techniques such as specific heat, tunneling spectroscopy, and measuring the penetration depth. However, this does not mean that there is a two-component superconductivity. In 2011, Karakozov *et al* discussed the temperature dependence of the magnitude of the superconducting gap normalized by that at 0 K in the two-band case [88]. It is well-described by the temperature dependence of that for an isotropic single gap for both bands in a two-band superconductor when the interband interaction is strong. This means that the Ginzburg–Landau formalism works well where the usual Ginzburg–Landau formalism has only one order parameter. There are two gaps, but they can be expressed by a single-order parameter. The emergence of the superconductivity is due to a proximity in the band having a weak intraband interaction. Zhitomirsky and Rice explicitly mentioned this situation in their article in 2001 [89]. When the interband interaction also becomes weak, the gap evolution in the weaker band deviates, although the gap evolution in the stronger band can be still reproduced by that of an isotropic single gap, as theoretically shown by Kogan, Martin, and Prozorov [90]. Karakozov *et al* stressed mainly this point and discussed the correction due to a weak interband interaction for MgB_2 and $Ba(Fe_{0.925}Co_{0.075})_2As_2$ [88]. Agterberg, Rice, and Sigrist discussed this situation for Sr_2RuO_4 in 1997 [91]. The Ginzburg–Landau formalism should also be modified, as discussed by Golubov and Koshelev [92]. A group from Antwerp University and Bayreuth University achieved further refinements of the Ginzburg–Landau formalism for a two-band superconductor [93, 94].

In addition to pairing interactions, the role of a single-particle scattering by an impurity should be considered. A single-particle scattering averages the gap anisotropy [26]. The multiple gaps converge into a single gap owing to the strong scattering. To exhibit the multigap nature, a sample should be purified to eliminate all impurities for transition metal superconductors [26, 95–97]. Dirty superconductors tend to have a single gap. However, Golubov and Koshelev reported that MgB_2 can have two gaps under a strong intraband scattering because the interband scattering is weak [92]. The weak interband single-particle scattering is a necessary condition to realize the two-gap situation, whereas the weak interband pairing interaction is a necessary condition to realize the two-component superconductivity. Only an isotropic s-wave superconductivity has a chance to emerge when the single-particle scattering ultimately works and totally

averages over the anisotropy in the dirty limit. Golubov and Koshelev's treatment is very convenient because an intraband isotropy is established by the strong intraband single-particle scattering, but we have still two gaps owing to a weak interband single-particle scattering. The sign-reversal situation, discussed by Kondo [62], needs a similar condition; otherwise, a gap is averaged and becomes small, which tends to destroy the superconductivity [98]. Now, we know that the d-wave superconductivity is realized in the cuprate superconductor [99]. This particular example guarantees that the single-particle scattering does not always average out the sign-reversal anisotropy and that no exotic situation is excluded by the single-particle scattering average. It also assists the emergence of the multicomponent superconductivity based on the multiband superconductor.

3. Topics regarding the multicomponent superconductivity based on the multiband superconductor

3.1. Type 1.5 superconductivity

As in the previous section, we discuss two situations: a two-component superconductivity and a two-gap superconductivity. These directly relate to the discussion on a type 1.5 superconductivity. In this section, we briefly survey the superconductor from that viewpoint.

When the Ginzburg–Landau parameter, which is ratio of the magnetic penetration depth to the coherence length, is greater than $1/\sqrt{2}$, a vortex with a unit flux quantum can enter into a superconductor (type II superconductor); otherwise, it cannot enter (type I superconductor) [100]. In a type I superconductor, we observe a lamellar structure wherein a normal state domain (a sheet or lamellar) accompanying the magnetic flux separates the superconducting domains [101]. The normal domains tend to gather in the type I superconductor. When the superconducting condensate has two components with different coherent lengths, we can define different Ginzburg–Landau parameters individually for each band. When one of the Ginzburg–Landau parameters is greater than $1/\sqrt{2}$ and the other is less than $1/\sqrt{2}$, the normal domain tends to be the smaller domain in one component, but in the other component, the normal domain tends to be the larger domain. This causes the non-trivial structure. In 2009, Moshchalkov *et al* coined this situation as 'type 1.5 superconductivity,' in which there is an attractive inter-vortex force in addition to the usual repulsive inter-vortex interaction depending on the inter-vortex distance [53]. This situation had been previously discussed by Babaev and Seipth in 2005 [54]. This scheme is from the viewpoint of two-component superconductivity.

The key issue of this discussion is whether we can provide two different coherence lengths in one superconductor. In the 1980s, this was studied on the multilayer structure of a type II superconductor as a problem of the abnormal upturn of the upper critical field H_{c2} with decreasing temperature [102, 103]. It was motivated by a study of alternating stacks of superconductor and non-superconductor, such as the Nb/Cu multilayer, but also pertains to superlattices composed of two superconductors. According to Takahashi and Tachiki's work concerning the multilayer, H_{c2} is mainly governed by the component with the longer coherence length near T_c. With decreasing temperature, H_{c2} tends to be determined by the component with the shorter coherence length. Between these two limits, the upturn of H_{c2} is observed. This tendency was also absolutely reproduced in MgB_2 [104]. At a low temperature, the order parameter is modulated in the direction perpendicular to the layers in the stacking period in the multilayer system. Introducing two different coherence lengths is a natural consequence. The group from Antwerp University and Bayreuth University analyzed this situation for a two-band superconductor well. Except precisely at T_c, the Ginzburg–Landau formalism derived from a gap equation reproduces difference coherence lengths for two gaps adopting the higher order terms of $1-\frac{T}{Tc}$ [94].

However, Takahashi and Tachiki reported that 'in the vicinity of the transition temperature, the pair function is almost uniform in the direction of the vortices.' This suggests that the superconductivity behaves as a single-component superconductivity near T_c. Because the Moshchalkov group took an image of a vortex arrangement under a field-cooled situation (the sample was cooled under a magnetic field) [53, 105]. The behavior of the superconducting condensation near T_c should be considered. Experimentally, the field-cooled situation is unavoidable. To see the vortex arrangement under a low field, the field cooling is necessary. Otherwise, a vortex hardly enters the sample. Although we push the vortex into the sample under a low field, the vortex distribution is determined by the Bean critical-state model [106] rather than by the type 1.5 nature. We cannot apply a sufficiently high field to see the vortex arrangement using the Bitter decoration technique [107–109] or the scanning superconducting quantum interference device (SQUID) microscope technique [110]. The maximum field is limited by the spatial resolutions of these techniques. The multiplicity of the components at T_c is a crucial issue when the vortex arrangement is determined at T_c.

Kogan, Schmalian, and their collaborators discussed this matter for MgB_2 [111–113]. They argued 'two-order parameters in two-band superconductors vary on the same length scale'. This theoretical observation supports the opinion of Takahashi and Tachiki for the multilayer system at T_c. The vortex is an ordinary one, and there is no chance to gather at T_c.

Silaev and Babaev argued that the coherence lengths are not defined for each gap [114, 115]. Rather, the coherence length should be given for their combination. This effectively causes a disparity in the spatial variation of the two gaps and the temperature dependence of the magnitude of the two gaps. Roughly, there are at least two arrangements of the two gaps. In one arrangement, the two gaps have the same sign, like an s^{++}-wave. The other arrangement is sign reversed, like an $s^{\pm}$-wave. Even when the s^{++}-wave is a dominant-order parameter, the $s^{\pm}$-wave component is superposed around a vortex. The coherence length of the dominant component diverges at

T_c. However, that of another one keeps a finite value of the coherence length. The magnitude of order parameter vanishes instead. The type 1.5 superconductivity can appear at T_c. The conventional Ginzburg–Landau formalism is composed of only the dominant component; here, it is the s^{++}-wave. The amplitude and phase dynamics of the s^{++}-wave can be treated by the conventional Ginzburg–Landau formalism, but a mixture of the $s^{\pm}$-wave cannot. The researchers are currently refining their idea and expanding to other multiband superconductivities [116, 117]. The superposition of the other component (such as an s-wave component) was actively discussed as the d-wave superconductivity in 1990s [118–124]. Hu and Wang indicated that it is difficult to describe the frustrated chiral superconductor, which is discussed later, by a single-component Ginzburg–Laudau formalism, because there are multiple divergent lengths of the superconductivity coherence [125]. This can be considered an extension of the type 1.5 superconductivity from the viewpoint of the number of coherence lengths.

The discussion of Kogan and his collaborators and that of Babaev and his collaborators relate not only to the justification of the type 1.5 superconductivity at T_c but to the physics of the phase transition of the multiband superconductor itself, directly. Briefly, Kogan's discussion based on the traditional superconducting science originating from the BCS theory where the quasi-particles convert into the pair with null entropy. (Of course, Kogan and his collaborators seem not to compeltely negate the entropy of the pair, giving rise to the Leggett mode.) Babaev put his foundation on the field theory [64, 67, 126, 127]. The fields (order parameters) are already there, and the fluctuation of this field (that is, the entropy of the pair) plays a major role. The unification of these two views is necessary to understand the superconducting phase transition of a two-component superconductivity based on two-band superconductors, i.e., whether it is the same as that of a single-component superconductivity or is drastically altered. We will return to this issue later.

3.2. Leggett mode

The identification of the excitation spectrum is the foundation of the BCS theory [128]. It is a pair-breaking excitation. The gap equation at T_c is given by the trade-off between the profit from the formation of a superconducting gap and the cost of the missing entropy of the single particle incurred by a pair formation. This is because the free energy is the sum of the internal energy U and the entropy S, which are related by $F = U - TS$, where T is the temperature. The pair does not have any entropy. The collective excitation and fluctuation of the pair are neglected.

The Leggett mode is the fluctuation in the relative phase and the pair density fluctuation between two bands. It is a collective excitation; this was neglected by the original BCS theory.

There were discussions about the collective excitation immediately after BCS theory. Anderson discussed two classes of excitations [129]. The first is a plasmon, which is a basically the same as that in a normal metal and the longitudinal density fluctuation of particles. The second is any bound pair having a wave function different from that of the pair in the ground state. A d-wave bound pair in an s-wave superconductor is one example. The long-range Coulomb interactions increase the energy of the former one far from the pair-breaking excitation. We need not consider this in the dynamics of the low-lying excitation near and lower than the pair-breaking excitation, except for the intrinsic Josephson plasma in the layered cuprate superconductor, which can be regarded as an in-gap excitation [130]. Anderson [129] and Richayzen [131] estimate the excitation energy of a bound pair in the latter case. Those excitation energies tend to be near the pair-breaking excitation. It was generally concluded that the excited bound-pair state rapidly decays into two unpaired fermions. The presence of these bound states never alters the basic properties according to the BCS theory, such as the opening gap at T_c with simultaneous evolution on any wave vector near the Fermi surfaces. Expectedly, there were some reports of these collective excitations, e.g., the theoretical discussion by Tsuneto regarding the in-gap state composed of a d-wave pairing in an s-wave superconductor [132]. There have been experiments to examine the collective excitation under the coupling with other order parameter, such as a charge density wave [133, 134], and the collective excitation excited by a very strong illumination [135, 136].

The starting point of the Leggett mode, in principle from these considerations, takes into account the collective excitation again [28]. In Anderson's discussion, the ground state of the superconductivity is composed of the s-wave pairing with the lowest orbital angular momentum and the highest symmetry. The excited bound state has a greater angular momentum and different symmetry. Leggett discussed the mixing of the excited bound state, where its symmetry is the same as that of the pairs of the ground state. The mixing of the excited state is effectively described by the interband phase difference fluctuation and the interband pair density fluctuation. Leggett considered that when the interband interaction is weak, the collective excitation lies well below the pair-breaking excitation.

Roughly, there are three viewpoints to explore the Leggett mode. On the first and most popular view, each of the bands has its own condensate. The condensate of one band weakly couples that of another band through an interband Josephson interaction. This viewpoint is instructive and intuitive. The similarity and analogy to other systems, including field theory [67], multicomponent superconductivity [137], and other multiple-order-parameters systems can be easily stimulated [13]. The second viewpoint is that a pair has an internal freedom originating from the band structure. On this viewpoint, the fluctuation of the Leggett mode gives some entropy to a BCS pair, which had been neglected to derive a gap equation and T_c in the original BCS theory. On the third view, the system is in principle a double-order-parameter system [137]. As discussed in the standard textbook [99], when there are two order parameters that can both be expressed by a single complex number, and the two order parameters have the same symmetry, the Ginzburg–Landau formalism requires us firstly to eliminate the quadratic

term at T_c, i.e., the inter-order-parameter Josephson term, by completing the square. In this procedure, the system is reduced to a single-order-parameter system, wherein the new single-order parameter is described by a linear combination of the original order parameters. The other linear combination can be installed to restore the freedom lost by completing the square, but it should be omitted at T_c. To introduce two different coherence lengths for the condensates on the two bands at T_c, the reinstallation of the omitted combination is necessary.

These three viewpoints do not differ significantly. The consequence of this description is revisited in section 3.5, with regard to the phase transition of the multiband superconductivity on the frustrated multiband superconductor.

The Leggett mode due to the weak interband interaction has long been experimentally and theoretically investigated. Griffin performed a theoretical analysis of the Leggett mode of multilayer cuprate superconductors [138], whereby the interlayer phase difference modes and other amplitude modes were determined. The researchers predicted that these features should be found in the Raman spectra. Kon, Ciobanu, and D F Digor theoretically calculated the Raman spectra of the two-band superconductor [139]. They reported a sharp peak, corresponding to the Leggett mode, due to the BCS pair interaction below the pair-breaking continuum. Both of the groups' theoretical calculations indicate the strong feature due to the interband phase difference fluctuation in the Raman scattering. The collective excitation in the multiband superconductor was also examined theoretically by Kochorbé and Palistrant [140]. Hadjiev *et al* [141, 142]. Limonov *et al* [143], and Tanaka *et al* [144, 145] measured the Raman spectra of the multilayer cuprate superconductor. They reported a strong electronic excitation continuum around and below the superconducting gap, which is not observed in the mono- and double-layer cuprate superconductors. Limonov reported that these electronic continua have a strong resonant property against the photon-exciting energy of a laser. The frequencies of some phonons are significantly changed below T_c, and those intensities are enhanced. The continua are found in multilayer cuprate superconductors having three or more CuO_2 planes per unit cell. The laser may induce the interband density fluctuation, which may not occur in mono- and double-layer cuprate superconductors. The strong electronic continuum and anomalous behavior of the phonon feature may relate to the Leggett mode.

Blumberg *et al* reported the Leggett mode in the Raman spectra of MgB_2 [146, 147]. This is currently the clearest evidence of the Leggett mode. Klein refined the Raman scattering theory for this experiment [148]. Chubukov, Eremin, and Korshunov tuned the Raman theory for pnictide to identify the gap symmetry, e.g., a d-wave, an s-wave, or an extended s-wave [149].

There is an experimental report of the Leggett mode using tunneling spectroscopy [150]. The Leggett mode would be excited at the interface of the multiband superconductor. Some theoretical reports are available [151–153]. The nontrivial interband phase structure is expected at the interface between a single-component superconductor and the two-band superconductor in which the interband phase difference is π radians in the bulk limit, which is called an $s^{\pm}$-wave superconductor when the symmetry of the order parameter is the same as that of an s-wave [20, 154–156]. According to the theoretical studies, we can identify an $s^{\pm}$-wave superconductor using tunneling spectroscopy. The three-band and four-band superconductors expected have far richer Leggett modes, as discussed later [47, 48, 51, 157–160].

3.3. Interband phase-difference soliton (*i*-soliton)

The interband phase difference fluctuation of the Leggett mode is considered to be very small. If this interband phase difference rotates by 2π radians when moving from one location to another location, there is a soliton in between [20, 21]. This is the interband phase-difference soliton (*i*-soliton). It is illustrated in figure 1. A soliton is generally expected to appear when there is freedom corresponding to the rotation [161, 162]. To form a soliton, we rotate internal variables. A magnetic domain wall [107, 108] can be considered one such soliton, in which the direction of the magnetic moment rotates, e.g., the Bloch wall [163]. Maki discussed a soliton structure in a ^{3}He superfluid [164, 165]. The soliton forms by undergoing a relative rotation between a spin coordinate and an orbital coordinate in superfluid ^{3}He-B. The rotation of the orbital wave function and spin of the pair also become a soliton structure in the superfluid ^{3}He-A. For the triplet superconductor, the soliton in the superconducting state having two degenerate components was discussed [137, 166]. In this soliton, the relative phase between the two components rotates. For a weakly coupled two-component alkaline atomic gas condensate in which there are two species with different total angular momenta (the two species are the same element), Son, Stephane *et al* discuss a soliton as a domain wall [167]. The two components are coupled by the laser illumination [168, 169], which corresponds to the Josephson interspecies interaction and is controllable in this system.

The *i*-soliton was discussed for the multilayer cuprate superconductor Cu-1234 [33]. As described before, NMR and specific heat studies indicated that Cu-1234 has a weak interband interaction, although its intraband pair interactions are considered to be strong [35, 36, 170]. The interband interaction is basically the pairing interaction on the one CuO_2 plane and the band structure considered to comprise the linear combination of the electronic structure of four CuO_2 planes [34]. We can tune the intrinsic T_c, i.e., the hypothetical T_c, while turning off the interband Josephson interaction by doping a hole into a selected CuO_2 plane [171]. It is confirmed by the vanishing of the anomaly in the irreversible fields [172] and the Knight shift in NMR [173] corresponds to the lower intrinsic T_c by the selective doping. We can consider that each band has strong intraband interactions. Crisan *et al* reported an indirect indication of the appearance of the vortex molecule related to the formation of the *i*-soliton in $CuBa_2Ca_2Cu_3O_y$ (Cu-1223) [37], which is one of the multilayer cuprate superconductors, as discussed before.

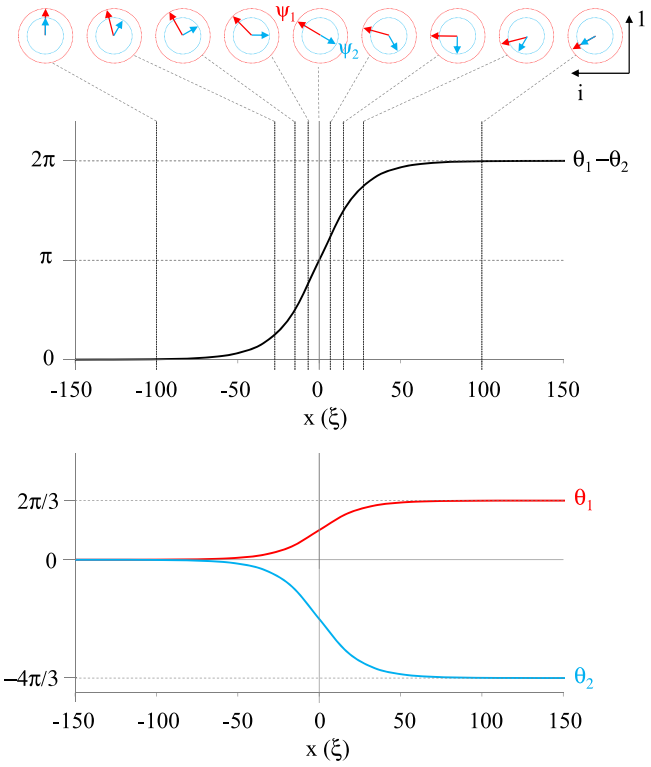

Figure 1. Schematic of an interband phase difference soliton in a two-component superconductivity based on a two-band superconductor. The ratio of the pair density of the first component (denoted by ψ_1) to that of the second component (denoted by ψ_2) is 2 to 1. The ratio of the condensation energy due to the intraband pair interaction to that due to the interband interaction is 20 to 1. The effective mass and coherence length are equal between bands. The arrow shows the arrangement of the components of the order parameters in the complex plane. The axes of the complex planes are denoted at the lower right of the upper panel. The magnitude of arrows does not have a definite meaning. The circles are included as a visual aid. The upper panel shows the variation of the order parameter. The middle panel shows the variation of the relative phase. The horizontal axis is the location in the units of the coherence length ξ. The bottom panel shows the variations of each component. The relative phase rotates by 2π radians. The phase shift is observed as $\pi/3$ radians in this example. The rotation is reversed, and the phase shift becomes $-\pi/3$ radians in an anti-*i*-soliton for this example. The phase shift depends on the ratio of the pair density and effective mass as the total current becomes zero. The length of the soliton is inversely proportional to the square root of the contribution of the condensation energy due to the interband Josephson interaction.

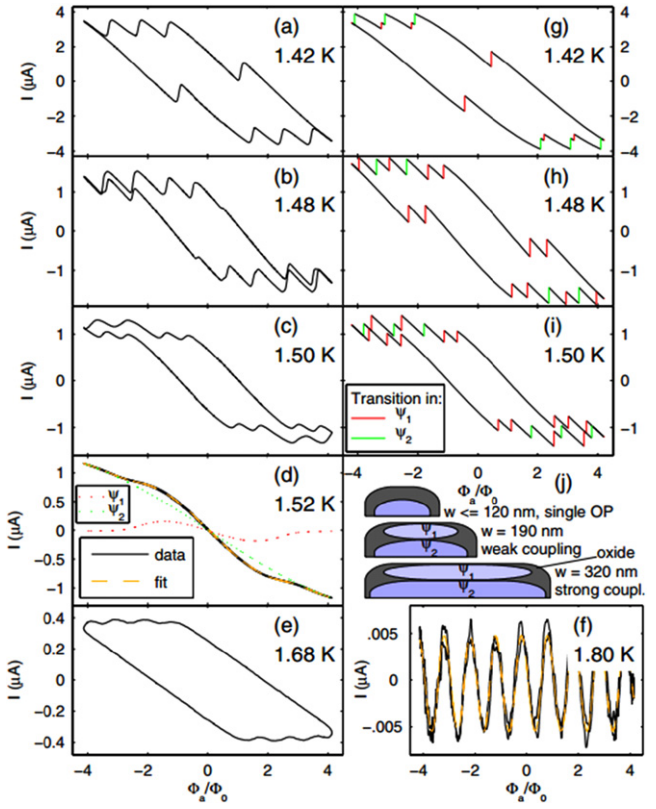

Figure 2. (a)–(f) Φ_a—I curves for a ring with $w = 190$ nm and $R = 2\ \mu$m, where the coupling between the two order parameters is weak. In (a)–(c), states with two different fluxoid numbers lead to the observed transition pattern. In (d), no transition occurs because one component is stabilized by the other. Dotted lines show the contributions of ψ_1 and ψ_2 derived from the model. (e) and (f), taken above the lower T_c, reflect the response of a single order parameter. (g)–(i) Results from the two-OP model corresponding to (a)–(c). (j) Schematic of film structure (cross section). (Reprinted with permission from [42]. Copyright 2006 by the American Physical Society.)

The soliton itself was experimentally reported by the Stanford group as a fractionalization of the unit flux quantum (fluxoid) Φ_0 [42]. The researchers mimicked multiband superconductors using Al-bilayers sandwiching an AlO_x barrier. The sum of the thickness of the Al-layers and that of the barrier is smaller than the penetration depth. This structure effectively reproduces the two-component superconductivity. By varying the external field, the researchers measured an induced current in a ring made from their mimicked multiband superconductor. In the conventional superconductor, the induced current oscillates with varying the magnetic flux inside the ring, whose period is Φ_0. When an *i*-soliton enters the ring, this oscillation is disrupted. This interference was measured as shown in figure 2. We concisely explain its mechanism in the illustration of figure 3. The mechanism employs a common technique for generating the fractional vortex discussed in the next section. When a phase of one component rotates clockwise, the other phase of another component rotates anti-clockwise in the *i*-soliton (this is illustrated in the top panel of figure 1). The sum of the currents in two bands becomes zero when there is no magnetic field. The directions of the currents are anti-parallel. This current is a neutral flow composed of the charged flows. It is not a spatially conserved current such as a spin current [174], indicating that there is a divergent location and a convergent location. Instead of the rotation of the spin, the interband phase difference varies. There is also an interband pair hopping flow between the two bands due to the interband Josephson interaction (shown in the top panel of figure 4). It causes a circulating flow spreading over two bands such as is found in the Josephson vortex (fluxon) [175, 176] on the extended Josephson junction (the current pattern and phase are shown in figure 4). The *i*-soliton is considered a '*fluxless*

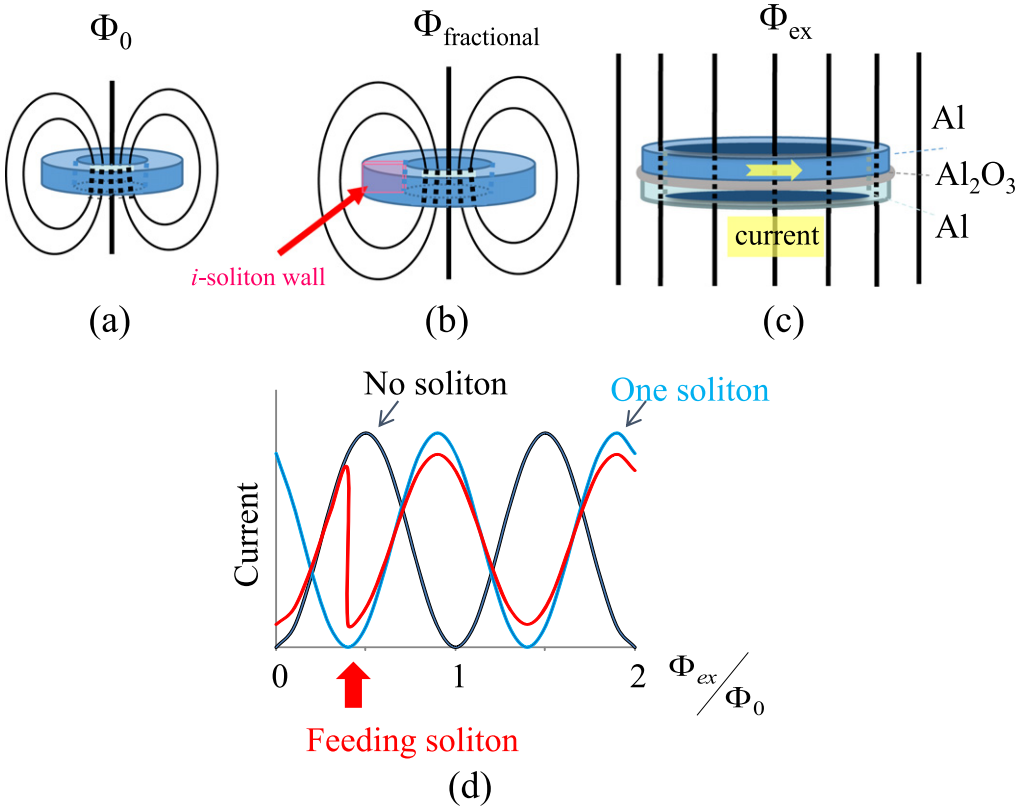

Figure 3. Schematic of the magnetic flux quantization of the ring made of superconductors. (a) The magnetic flux is quantized as Φ_0 for a usual superconductor. Φ_0 is a unit flux quantum. When the ring is thicker than the magnetic penetration depth, Φ_0 is trapped. (b) The fraction flux $\Phi_{fractional}$ is trapped when the *i*-soliton is fed in a multiband superconductor. The head and tail of the soliton along the ring. The line of the relative phase of π radians is along the radial direction of the ring. The relative phase variation described in figure 1 is observed along the perpendicular direction of the *i*-soliton wall. The sum of the phase shift due to the *i*-soliton and the phase shift due to the fractional flux, $-2\pi\Phi_{fractional}/\Phi_0$, becomes an integer. (c) The ring made of Al-bilayer, which is thinner than the magnetic penetration depth. The external magnetic field is homogeneously applied. The current inside the ring depends on the magnetic flux inside the ring and oscillates with a period of Φ_0 in a usual situation (d). When there is an *i*-soliton, the phase shift occurs, as shown in (d). When the number of the *i*-soliton in the ring changes, a jump in the current is expected.

fluxon'. At the tail of the *i*-soliton, the component rotating clockwise never meets another component rotating anti-clockwise with the same phase as that at the head of the *i*-soliton. There is a phase shift between the head and the tail of the *i*-soliton (shown in figure 1). In the ring geometry, this phase mismatch should be compensated by the vector potential accompanying the magnetic flux inside the ring (illustrated in figure 2(b)). Consequently, one component is rotated by 2π radians, and another is not. The magnitude of the flux does not become an integer multiple of the flux quantum Φ_0. A similar feature was observed in the θ–soliton, and a spin-mass vortex of ^{3}He-B condensates where the relative angle between the spin coordinate and the orbital coordinate of the pair rotates [177].

There is a difference in the phase and internal current flow between the Leggett mode and the *i*-soliton, as shown in figure 4. We can provide the circulating flow without coupling to the amplitude mode of the gap in the weak interband coupling limit in the *i*-soliton. In the Leggett mode, the pair tends to concentrate in one location of one band instantaneously. This instantaneous concentrated location is where the phase difference is maximum. Moreover, the pair tends to go the band, which has an advanced phase. In the standing wave, this concentrated location on the band becomes the deficient location on the band after a half-period of this Leggett mode. Then, we have a time oscillation of the amplitude of the gap or the pair density at the anti-node location. Making an *i*-soliton, we can, in principle, decouple the amplitude mode and the interband phase difference mode. Consequently, the *i*-soliton is electromagnetically inactive [20–22]. To detect it, we must extract the magnetic properties using a topology such as the ring employed by the Stanford group [42].

Because the *i*-soliton is electromagnetically inactive, its generation and detection cannot be achieved using the conventional transport technique. Gurevich and Vinokur proposed a non-equilibrium current injection to generate the *i*-soliton [22]. This is analogous to the generation of the fluxon in an extended junction [178–180]. We apply a larger current exceeding the Josephson critical current between two banks sandwiching the interface to generate a fluxon in the case of the extended junction. Thus, current can never flow from one bank to another bank straightforwardly. It snakes and finally forms a circulating flow spreading over the two banks, and it

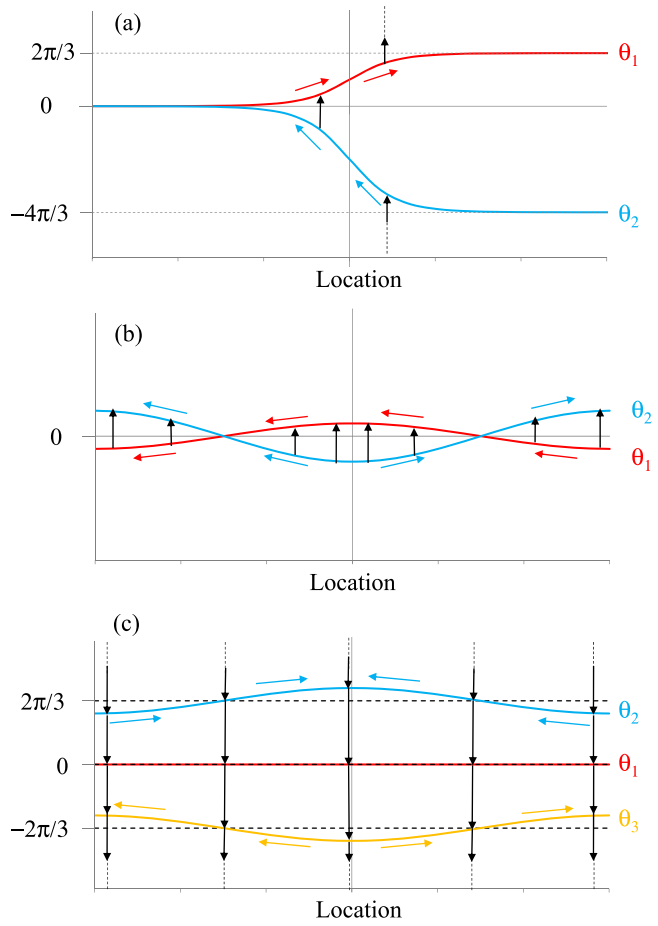

Figure 4. Schematic of the phase variation in an *i*-soliton in a two-component superconducting condensate: (a) Leggett mode in a two-component superconducting condensate, and (b) Leggett mode in a frustrated three-component superconducting condensate. A static structure is presented in (a). Dynamic structures such as a standing wave are presented in (b) and (c). The incline arrows indicate intra-component pair flows. Their horizontal component schematically shows the direction of the flow, while the vertical arrows indicate the interband pair hopping. In the frustrated situation, the direction of the pair hopping is reversed. We observe the circulating flow in (a) and (c) but not in (b). In principle, we can imagine the decoupling between the amplitude mode of the order parameter and the phase mode in (a) and (c). In (b), the coupling of the two modes may be inevitable.

then starts to leave the electrodes. Gurevich and Vinokur replaced the bands with banks (two superconducting layers). According to their proposal, an imbalanced injection is inevitable when the current is applied from the electrodes into a two-band superconductor because the achievement of a balanced injection is far more difficult. (The imbalanced injection from one electrode corresponds to applying the current between the two banks in the extended junction.) A similar circulating current flow occurs, as seen in the fluxon in the extended junction when the current exceeds the threshold corresponding to the Josephson critical current of the extended junction. The circulating current flow, is a property of the *i*-soliton, but the carrying of a fluxoid is not. The *i*-soliton has its anti-object; in the anti-*i*-soliton, the rotation of the interband phase difference is reversed. In the Gurevich and Vinokur circuits, there are two electrodes at the two ends of the sample. The *i*-soliton is generated at one end, and the anti-*i*-soliton is generated at the other end. Then, the *i*-soliton and the anti-*i*-soliton meet at the center and annihilate. The voltage generated by the annihilation should be detected. The researchers extended this idea to the mimicked two-component superconductor composed of a thin superconducting bilayer [181].

We must overcome an experimental difficulty to realize Gurevich and Vinokur's proposal. Gurevich and Vinokur showed that the *i*-soliton wall was generated like a bubble under the electrode. The electrode should cover the width of a line when we want to push the soliton into a line. When we put the electrode on a corner of the sample, we cannot apply enough energy to grow the soliton wall spanning both sides of the line and traveling inside the sample, leaving the electrode.

This condition had been experimentally examined before Gurevich and Vinokur's proposal by Kopelevich *et al* in 1998 for a different aim [182]. After some discussions [183, 184], they reported that it is difficult to achieve homogeneous current distribution and equipotential condition under the electrode pad [185]. Their objectives were the generation of the vortex and anti-vortex pair and its travel into the line near T_c. Their method can be applied on Gurevich and Vinokur's soliton emitter at a low temperature if it is sufficiently improved to eliminate the unwelcome effect from non-equipotential situations by good homogenous ohmic contact with a low-contact resistance at the electrodes.

There is another study about the *i*-soltion formation inside the superconductor caused by the large current density (not by the non-equilibrium current injection). This is the extension of the timewise oscillation of the superconducting phase at a phase-slip center, which occurs at a weak link under a resistive state, owing to the cyclic breakdown and recovering of superconductivity [186]. Yerin, Fenchenko, and their collaborators applied their own numerical approach [187, 188] for the superconducting filament on the two-band superconductor MgB_2 in pursuit of an *i*-soliton like texture. They observed no interband phase difference under a direct current (DC) [189]. They are currently extending their method for an alternating current (AC) [190].

Yerin, Omel'yanchuk, and their collaborators also attempted the *i*-soliton formation at the ground state or by fluctuation in a thin wall or narrow lines. Their formalism includes a drag effect between two condensates. Roughly speaking, the drag effect describes an effect by which two condensates tend to flow in the same direction. Mathematically, it is a cross term of the kinetic term of the Ginzburg–Landau equation [127]. (This term also appeared in the discussion about the anisotropic superconductor having different effective masses along three spatial coordinates and can be dropped by the diagonalization of the mass matrix [191].) They sought the *i*-soliton formation theoretically by their phenomenological Ginzburg–Landau formalism [68], although introducing the drag effect tends to make the *i*-soliton formation difficult because the components flow in anti-parallel directions, yielding a neutral flow in the *i*-soliton, as described before. According to their theory, the Little–

Parks oscillation [192, 193], which is the periodic oscillation of the T_c of the superconductor ring under a varying external field, in the two-band superconductor is the same as that of a conventional single-component superconductor [194]. There is no influence originating from the *i*-soliton. They sought to determine the trace of the soliton. Little and Parks measured the resistivity immediately below T_c instead of measuring the oscillation of T_c in their original work, because the variation in T_c is too small to be measured properly. The Stanford group measured the current in the ring rather than measuring the resistivity [195]. The current is measured using an inductively coupled ring, without making contact, to eliminate the influence of the electrode. The experiment performed by the Stanford group was an ideal Little–Parks experiment. After the Stanford group discovered the *i*-soliton in the ring composed of a two-component superconductor [42], Kuplevakhsky, Omelyanchouk, and Yerin refined their theory and discovered that the *i*-soliton has a chance to appear in the mesoscopic ring made of a superconducting bilayer, in general [196]. They also mentioned the formed *i*-soliton can move freely in the ring, causing zero-frequency rotational motion. Tanaka *et al*, in their patent, proposed to devise a shrunken location to stop this motion and pin the *i*-soliton at a desired location [17]. Vakaryuk *et al* proposed that placing a superconductor having a different symmetry order parameter on the ring decreases the *i*-soliton formation energy in the ring. The proximity of the different-symmetry-order parameter to the ring weakens the superconductivity locally. The *i*-soliton is trapped at that location. Smorkhin theoretically showed that the formation of the soliton can be also detected by tunneling spectroscopy as a density of the state of the quasi-particles trapped by the *i*-soliton [197]. This technique provides another method in addition to measuring the flux inside the ring and the current, and it is useful for the detection of the *i*-soliton in open circuits.

3.4. Fractional flux quanta

3.4.1. Topology. The fractional vortex is generated when the *i*-soliton attaches to the vortex, because the *i*-soliton changes the quantization condition of the magnetic flux by the accompanying phase shift, which is hidden from the electromagnetic field. Here, a 'fractional vortex' is a vortex carrying the fractional flux quanta [45]. This mechanism is identical to the fractionalization of a unit flux quantum inside the ring, as discussed in the previous section. A fractional vortex in the multicomponent superconductivity corresponds to a spin vortex in ^{3}He-B [177]. A fractionalization of the unit flux quantum is also seen in the half-integer fluxoid generated at the grain boundary junction formed by the d-wave superconductor [198, 199]. The current circulating around the vortex passes two junctions. These two junctions are designed so as to change the sign of the pair tunneling matrix element using the anti-symmetry of the d-wave symmetry by the mirror reflection on the plane that is a bisector of an angle defined by an *a*-axis and a *b*-axis. The π-radian phase shift occurs owing to this junction, and a vector potential of a half-integer fluxoid compensates this phase shift. The π-radian phase shift corresponds to the phase shift due to the *i*-soliton. There is a half-integer flux in triplet p-wave superconductors as well [166, 200, 201]. The half-integer vortex appears on the chiral domain wall. The circulating current passes the chiral domain wall twice. The chiral state can be represented by two components having a relative phase of $\pi/2$ radians [137]. One pass rotates the phase of the first component by $\pi/2$ radians, the phase of the second component by $-\pi/2$ radians, and the relative phase by π radians. The second pass rotates the phases similarly. Finally, the relative phase is rotated by 2π radians, but the phase shift of each component becomes π radians. The vector potential accompanied by the half-integer fluxoid compensates this phase shift of π radians. The *i*-soliton has the same function as two chiral domain walls in the p-wave triplet superconductor on the phase shift.

The difference in the phase shift due to the domain walls [9, 51, 202–204] is indicated in figure 5, including the case of a frustrated superconductivity, which is discussed later.

3.4.2. Formation of the fractional vortex. From the topological viewpoint, the fractional vortex is accompanied by the *i*-soliton. Because the *i*-soliton formation must have a cost, we account the energy balance to consider the fractional vortex formation. We summarize the four ways to form the fractional vortex in this section.

3.4.2.1. Energy balance between the Josephson energy and magnetic energy. Primarily, the fractional vortex formation is a result of the trade-off between the cost of the interband Josephson energy and the gain from the magnetic energy [38]. The magnetic energy is minimized when the distribution of the magnetic flux is homogeneous. The magnetic flux distribution is divided into fragments as small as possible when there is a superconductor to inhibit this homogeneous distribution. Simultaneously, owing to the phase connectivity of the superconductor, because the phase couples with the vector potential, the vortex having the unit flux quantum appears. When further fractionalization decreases the magnetic energy and its gain exceeds the cost of the interband Josephson energy, the fractional vortex appears. If we adopt this principle to realize the fractional vortex, the resulting mesoscopic structure is ideal, i.e., appropriate for reducing the Josephson energy. Subdividing the flux quanta reduces the magnetic energy in the mesoscopic structure. The *i*-soliton wall terminates at the edge of the sample. Then, the cost of the *i*-soliton formation energy can be reduced in the mesoscopic structure [205–212]. The approach for the half-integer vortex of Sr_2RuO_4 follows the same principle [201].

The *i*-soliton formation energy can also be reduced by the termination of two fractional vortices. This is a vortex molecule (figure 6), which is composed of two fractional vortices bridged by the *i*-soliton. The phase of the first component rotates by 2π radians, but that of the other component does not rotate around the core for the first fractional vortex. This is a single winding vortex. In another fractional vortex, the phase of the second component rotates

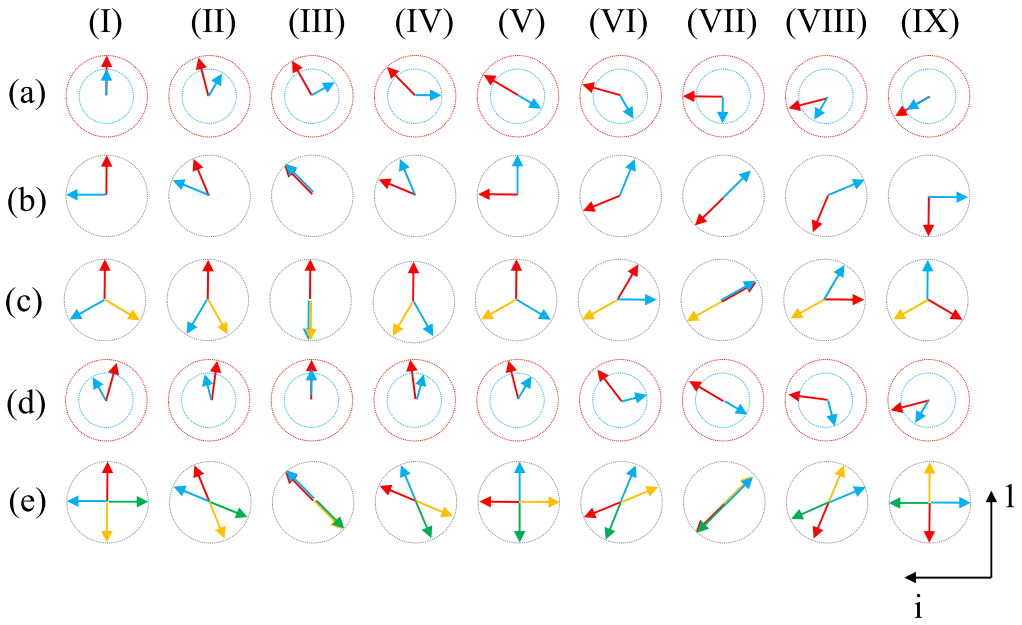

Figure 5. Order parameter arrangements for an *i*-soliton, (a) in a two-non-degenerated-component superconducting condensate, (b) in a chiral superconducting condensate composed of doubly degenerated components, (c) in the frustrated three-component superconducting condensate, (d) in a chiral superconducting condensate composed of two non-degenerated components, and (e) in the frustrated four-component superconducting condensate. (I)–(IX) Indicate locations. In (c) and (e), the equivalent bands are provided. The same situation is expected in the non-equivalent situation for (c). The phase shift is observed between (I) and (IX). The *i*-soliton is formed by a continuous change from (I) to (IX) in (a). (I) and (V) of (b)–(d) are degenerated chiral states. The chiral domain wall is formed by a continuous change from (I) to (V) or (V) to (IV) in cases (b)–(d). The continuous change (I)–(IX) for (e) gives the same energy. It becomes a massless mode.

by 2π radians, but that of the first one does not. When the contribution of the interband interaction to the superconducting condensation energy becomes less than approximately 5% of the intraband interaction, the vortex molecule forms [38]. The vortex molecule can be detected by the macroscopic technique. There is a new freedom that the ordinary cylindrical vortex tube does not have (shown in figure 6(a)). The vortex molecule can turn along the direction of the magnetic field, and this rotational motion can be detected. The vortex lattice melting by the translational motion perpendicular to the axis of the vortex is well-studied for the cuprate superconductor [213]. We can measure the loss due to the vortex translational motion above the melting temperature in the situation illustrated in figure 6(b) by the AC magnetization [214, 215]. Similarly, we can measure the loss due to the vortex molecule rotation. Crisan *et al* reported the signal indicating the rotation of the vortex molecule in the multilayer cuprate superconductor Cu-1223 (figure 7(a)) [37]. Shivagen *et al* discovered scaling phenomena in the frequency dependence of the out-of-phase component of the AC magnetization by varying the temperature (figures 7(b) and (c)) [39]. The scaling behavior can be considered as the consequence of the critical slowing down of the rotational motion [216–218].

The fractional vortices are confined within the vortex molecule because an isolated fractional vortex should have an *i*-soliton tail and another end of this *i*-soliton tail should be terminated by an edge of a sample or another fractional vortex as seen in the spin-mass vortex [177] in a ^{3}He-B condensate and a quark in a hadron [6, 18, 66, 219, 220]. The energy of the *i*-soliton is proportional to its length, where the rotation of the interband phase difference is observed as perpendicular to the *i*-soliton tail. When the interband interaction is not too weak, two fractional vortices coaxially overlap and form a composite vortex. This composite vortex is an ordinary vortex, as indicated by transmission electron microscopy in MgB_2 [221]. There is another principle involved in decomposing the composite vortex, which we introduce in the next section.

3.4.2.2. Thermal decoupling of the composite vortex. The second principle pertaining to the formation of the fractional vortex is the gain in the free energy of the entropy of the *i*-soliton. The *i*-soliton is considered as the domain wall. The domain wall can be bended and is deformable. The variation in the deformation of the *i*-soliton contributes to the generation of entropy. When this entropy exceeds the cost of the formation of the *i*-soliton, the *i*-soliton is invoked, causing the fractional vortex [219, 222, 223]. This is the dissociation of the vortex, and it is expected to occur near T_c. When a single winding vortex dissociates by the formation of the *i*-soliton induced by the entropy, it becomes a fractional vortex and carries a fractional flux quanta. Babaev suggested that there would be a formation of a pair of a fractional vortex and an anti-fractional vortex in a two-dimensional system [45], as observed in the formation of a pair of a vortex and an anti-vortex below the Berezinskii–Kosterlitz–Thouless (BKT) transition [224–226]. This mechanism is similar to that examined by Goryo *et al* when a composite vortex can dissociate, a pair comprising the antivortex and vortex can

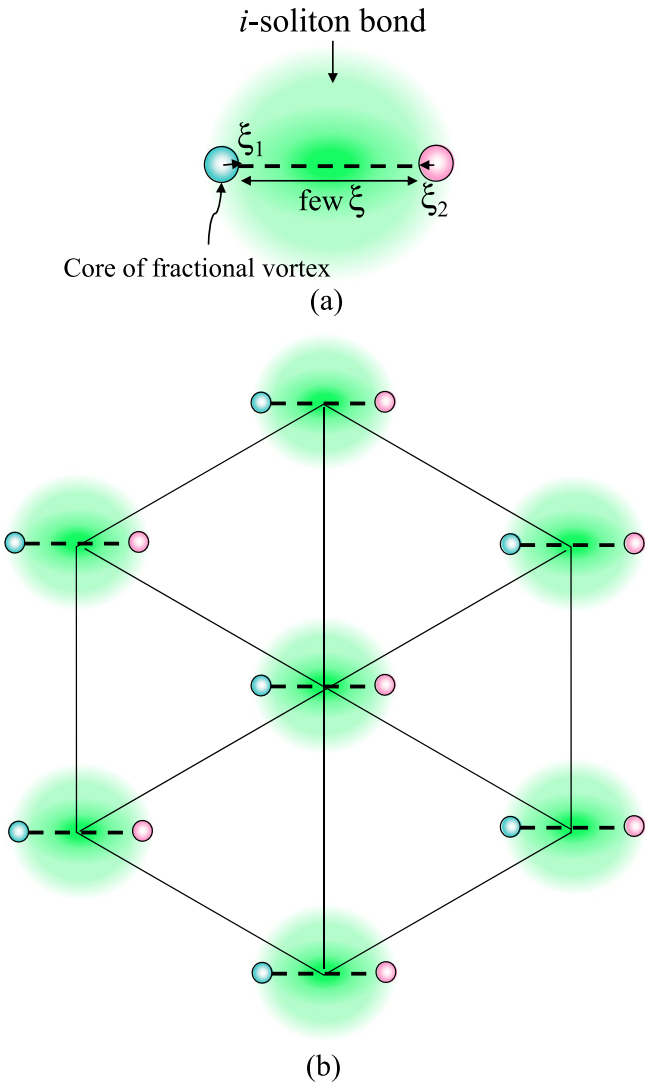

Figure 6. (a) Schematic of the vortex molecule that is suggested to emerge in Cu-1223. The blue and pink balls indicate the cores of each component. The green cloud indicates an *i*-soliton. The broken line indicates the region where the phase difference becomes π radians. (b) Schematic picture of the vortex molecule lattice. The vortex molecule can rotate as well as perform a translational movement.

form because the vacuum having no vortex can be considered as the condensation of the vortex having a winding number of zero. The formation of the anti-vortex and the vortex can be considered as the dissociation of the vortex with a winding number of zero. The Uppsala University group and a Korean researcher attempted to determine the noise due to this formation of the pair of the anti-vortex and the vortex in MgB_2. They detected something, but seeing that it might be due to the pair formation, their report seems inconclusive.

The dissociation of the vortex is considered in the pancake vortex array in a multilayer structure as the vacancy of the single pancake vortex [223]. In the layered structure in which the layers are weakly coupled by the interlayer Josephson interaction, the vortices are confined in each layer, and they stack along the magnetic field direction. This is an array of pancake vortices. If one of the vortices is missing, it

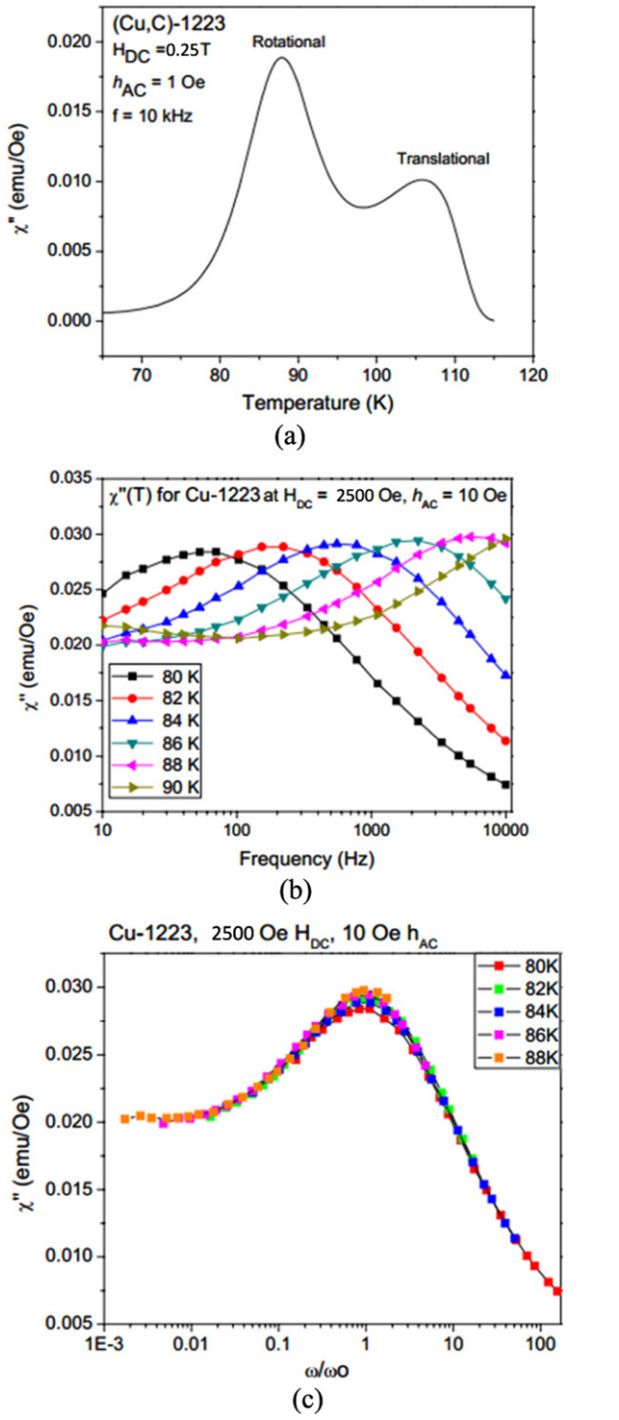

Figure 7. AC magnetization of Cu-1223. The magnitude of the DC applied field is halved because the magnitude in the original report reflected an error in the magnitude of the DC applied magnetic field owing to machine trouble [38]. (a) The temperature dependence of $\chi''(T)$ on aligned (Cu, C)-1223 crystallites under DC magnetic field of 0.25 T. The higher temperature peak is assigned to the dissipation due to the translational motion of the flux lines. The lower-temperature peak is assigned to the dissipation due to the possible rotational motion of the vortex molecule. (b) Frequency dependence of $\chi''(T)$ at DC field of 0.25 T, in the temperature range of lower temperature dissipation peak, giving resonance peak. (c) Scaling of frequency dependence of $\chi''(T)$ at DC field of 0.25 T in the temperature range of second dissipation peak, using individual resonance frequencies. (Reprinted with permission from [39]. Copyright 2008 by IOP Publishing).

becomes the fractional vortex. Under a higher field, the array along the magnetic field is destroyed. This is known as a three-dimensional to two-dimensional (3D-2D) crossover [227–229]. In this situation, the repulsive interaction between the pancake vortices in the same layer dominates, exceeding the cost of the interlayer Josephson interaction due to the interlayer phase difference. The array of the pancake vortex is also destroyed at high temperatures and by the absence of the Josephson interaction in the layered system [230–234]. These are well-discussed for the cuprate superconductor and a multilayer made of conventional superconductors. The physics of the vortex dissociation in the multiband superconductor and the vortex lattice melting of the multilayer may be unified.

3.4.2.3. Suppression of another component owing to a positive interaction. The third principle of the formation of a single winding vortex is the repulsive interaction between components. This is shown in the ^{3}He superfluid [235] and multicomponent Bose–Einstein condensates of the atomic gas [56]. When there is a repulsive interaction between two components, the second component tends to sit on the core of the vortex of the first component. This distribution lowers the interaction energy.

This exclusive distribution was utilized to form the vortex in the Bose–Einstein condensate of the atomic gas by the Joint Institute for Laboratory Astrophysics (JILA) at the University of Colorado in 1999 [56]. The formed vortex was a single-component winding vortex in which one component made a vortex and the other component was distributed in the core of the first vortex and did not make a vortex. The role of the non-rotating second component at the core is the pinning center of the single winding vortex of the first component. Doi and Natsume theoretically analyzed a single-component winding vortex [236]. Kasamatsu *et al* theoretically showed the vortex molecule and the fractional vortex lattice in which the core of the single-component winding vortex was between the core of the other component [237]. The stepping away of the core of one component from the core of another component is one consequence of exclusive distribution coming from the repulsive interaction. They also presented the phase diagram of the vortex lattice of the two-component Bose–Einstein condensate of the neutral boson [238]. In the Bose–Einstein condensates, the Josephson interaction between two components is achieved by the conversion of the total angular momentum of the atoms by the light (Rabi coupling) [168, 169]. The strength of the Josephson interaction varies with the intensity of the light, which determines the transition rate. Cipriani and Nitta theoretically showed that there are bound states for more than two fractional vortices, depending on the inter-component strength [239]. A vortex with more than two components, in which each component had a different winding number, was experimentally demonstrated in an extension of JILA's 1999 work [240].

This exclusive tendency due to the repulsive inter-component interaction may affect the fractionalization in the multicomponent superconductivity based on the multiband superconductor when there is a positive Josephson interaction, which tends to realize the π-radian phase difference between different components, as discussed in section 3.5. A precise and complicated fractionalization of the magnetic flux is frequently addressed theoretically in such systems [207, 241, 242].

3.4.2.4. Utilizing an external force and structure. The final way to decompose the normal vortex is by introducing the external fields: a pinning center, flux flow, matching field, manipulation by the ferromagnetic needle, and their combination. When we apply a current to the superconducting film perpendicular to the vortex axis, the Lorentz force is applied on the vortex. When the Lorentz force exceeds the pinning force, the vortex starts to move. This is a flux flow state, and it is readily occurs at a high temperature and current density [243]. Lin and Bulaevskii theoretically demonstrated the decomposition of the normal vortex into a fractional vortex in this flux flow state. The speed of the single-component vortex can change because of the difference in the viscosity of the vortex, which is determined by the size of a normal core of each component [244]. The abnormal viscosity was further discussed by Silaev and Babaev [245]. Silaev theoretically proposed that a fractional vortex can enter into a sample in a multicomponent superconducting state instead of a usual composite vortex [246], as the spin-mass vortex does in the ^{3}He-B condensate [177]. The dissociated vortex can be trapped by a pin, as Lin and Reinchhardt showed theoretically. They provided two holes for one flux quantum, which matches the number of fractional vortices [247]. The chip of the magnetic force microscope (MFM) is also effective. As a chip of a scanning tunneling microscope manipulates individual atoms [248], the Stanford group experimentally manipulated a fractional vortex using the chip of an MFM, which comprises a ferromagnetic needle [44]. The system is the ultra-underdoped $YBa_2Cu_3O_x$. This system is considered to be in the multicomponent superconductivity because the magnetic penetration depth is very large and the thickness of the sample becomes effectively smaller than the penetration depth. We illustrate a plausible situation for this system in figure 8. It is the same situation as was discussed before for the Al-bilayer system [42]. There are many fractional vortices in the system as it is [43]. Because it is difficult to remove the oxygen homogeneously, some interlayer couplings become very weak, whereas other interlayer couplings remain strong. The layers coupled by the strong interlayer coupling act as one component that couples to the other component through weak interlayer coupling. The Moler group suggested that there is a pinning center supporting the fractional vortex. This unintentional pinning center plays the role of the artificial pinning center proposed by Lin and Reichhardt. In the first stage, they accidentally discovered the spontaneous fusion of the fractional vortices into a normal vortex [43]. The experimental image of the fractional vortex fusion is

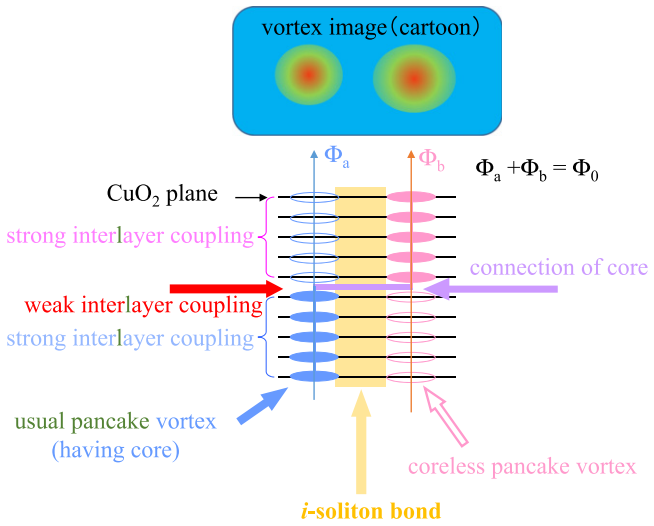

Figure 8. Schematic for one plausible situation of the fractional vortex formation in the cuprate superconductor. When there is a strong interlayer coupling and weak interlayer coupling, multi-component superconductivity can emerge. Each single winding vortex carries a fractional flux quanta indicated by Φ_a or Φ_b. The sum of these becomes Φ_0.

presented in figure 9. Subsequently, they utilized MFM to control the fusion and decomposition. The MFM technology enabled them to decompose the normal vortex into fractional vortices and to synthesize the normal vortex from the fractional vortices. It may be the most advanced and fruitful technology regarding fractional vortex matter in the field of multicomponent superconductivity. The Stanford group interpreted their results according to the theory of the magnetically coupled pancake vortices array, in which the interlayer Josephson interaction is neglected [230]. To interpret their results, there is another theory that was developed for the general case of the fractional vortices growing from the soliton wall introduced by the field theory of Kasamatsu *et al* [249]. It was originally developed for the two-component condensates of the neutral boson, but it can be applicable for the charged boson. These two theories can be unified because their physics are very similar from the viewpoint of the inter-component phase difference.

3.5. Interband phase difference frustration, gauge field, and massless mode of the relative phase difference; entropy of the pair

The *i*-soliton and the fractional vortex can be considered as consequences of the topology of the relative phase. These topological objects also appeared in the non-Abelian gauge field theory [66]. They have many commonalities with regard to physics. However, a simple extension of the field theory introduces the serious problem of the superconducting phase transition of the multiband superconductor. The filed theory, in principle, dose not treat the normal component, which comprises incoherent particles. Even in the Ginzburg–Landau formalism, the normal component reflects only the reduction in the amplitude of the order parameter and is not treated explicitly. In condensate physics, there is a popular model called the 'two-fluid model' [250–258] for treating the coherent portion and incoherent portion equivalently. In the two-fluid model, the system comprises the coherent condensates and a non-coherent normal component. In the case of the simple Bose–Einstein condensate, the coherence is achieved by the simple superposition of the lowest state of each boson. The interaction term is not necessary to form a condensate. In the case of the superconducting condensate, the interaction between normal particles makes the gap and the interaction between pairs necessary to achieve the condensate. The field theory does not distinguish between these two situations in principle. That is, the field theory does not definitely determine the properties of the phase transition; we must therefore introduce a complementary physics to support it. It is sometimes considered that the microscopic theory can fully provide the compliment supplement [259, 260]. Without a full *ab initio* calculation accounting for all of the freedoms of the electrons and atoms whose number is the Avogadro number, the description of the system remains imperfect. We use the trial function even in the microscopic calculation. If the trial function does not cover a situation of the system well, the result based on the microscopic theory does not describe the real system. On the other hand, the system is well-described when an appropriate trial function is adopted. The simplest trial function is sometimes better for revealing the transparent and intuitive physics than a complicated one. In this section, we seek the simplest origin and seeds with the potential to be beyond the conventional understanding of the superconductivity in the multicomponent superconductivity based on the multiband superconductor.

An interband phase difference between degenerate components is not locked without introducing an extra term that is not included in the BCS equation, when the BCS equation gives this degenerate solution [261]. The spin triplet p-wave state found in the ^{3}He condensate is one example. The phase difference of $\pi/2$ radians has been discussed in the triplet superconductivity for triplet superconductors such as UPt_3 and Sr_2RuO_4 [262] when there is a biquadratic term in the free energy [89, 137, 263]. The biquadratic term has a period of π radians. The energy minimum is given at either 0 or $\pi/2$ radians. The case of $\pi/2$ radians is known as the time-reversal-symmetry-broken state, denoted by $\Psi_1 + i\,\Psi_2$ where Ψ_i denotes ith component of the order parameter (all of Ψ_i have the same argument). Without the quadratic term, the general Ginzburg–Landau formalism with double order parameters has the same state in general owing to the biquadratic term [5]. The same situation has been discussed for mixing the degenerate components having difference symmetries in the cuprate superconductor, skutterudite superconductor, and pnictide superconductor [264–270], which is known as a (d + *i* s)-wave. This indicates the mixing of the d-wave and s-wave components. In the theoretical formalism, it appears to be caused by the biquadratic term or the local symmetry breaking around an impurity, a vortex, a surface, or an interface. When the biquadratic terms give the local minimum in the relative phase between 0 and π radians, the bulk time-reversal-symmetry-broken state is possible, as for

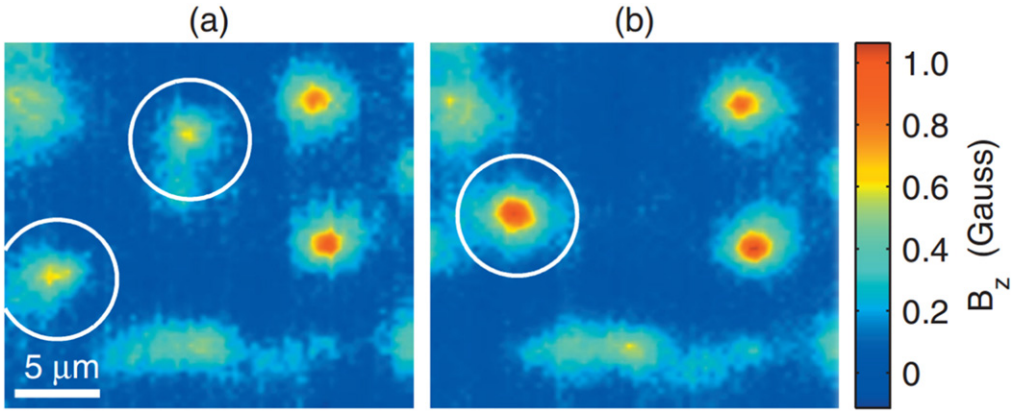

Figure 9. Vortex image of the ultra-underdoped $YBa_2Cu_3O_y$. Partial vortices coalesced during the sample coarse motion ($T = 2.4$ K). (a) Hall probe image after cooling through $Tc = 8.6$ K in the $Hz = 0.21$ Oe applied field. White circles identify two partial vortices. (b) After a slight z coarse motion of the sample. A comparison of the images suggests that the partial vortices in (a) collapsed to one full vortex in (b). (Reprinted with permission from [43]. Copyright 2008 by the American Physical Society.)

the degenerate double components system. Without the degenerate components or the mixing of different components having different symmetries, no mechanism had been discussed for time-reversal-symmetry breaking in the last century.

In 2001, Tanaka showed that the frustration can be another mechanism giving rise to the time-reversal-symmetry-broken state. This may happen at the interface between the two-component superconductivity and a single-component superconductivity, where the two-component superconductivity has the order parameter of the sign reversal, which is called an $s^{\pm}$-wave [20]. The relative phase difference between two components is π radians, and the total order parameter can be expressed as $\Psi_1 - \Psi_2$. At the interface, both components tend to have the same sign as that of a single-component superconductor. This gives rise to the interband phase difference instability in the two-component superconductivity, and the broken time-reversal-symmetry state occurs. Three-component superconductivity emerges at the interface, where the frustration triggers the time-reversal-symmetry breaking. This was also mentioned by Stanev and Tesanovicin 2010 [50]. The same situation was discussed by Ng and Nagaosa in 2007. A related topic was treated by Iniotakis, Fujimoto, and Sigrist [271]. Lin theoretically investigated this situation in detail [272]. Tanaka also discussed the broken time-reversal-symmetry bulk state under the co-existence of the attractive pair interaction and repulsive pair interaction, which is the origin of the frustration as one situation that may possibly occur in Cu-1234 [20]. The attractive pair interaction tends to scatter the pair without a change in the phase, i.e., scattering due to the conventional electron–phonon interaction. The repulsive interaction tends to scatter the pair with change of the sign. One example of this type of interaction is the exchange-like pair scattering discussed by Kondo [62, 273–278]. Another example is an interaction causing d-wave superconductivity in a cuprate superconductor [99].

Shirage *et al* experimentally revealed a competition between these positive and negative pair interactions in a pnictide superconductor [279]. They observed an inverse isotope effect in $(Ba,K)Fe_2As_2$. If the superconductivity was mediated by the electron–phonon interaction, T_c decreased with the increasing of mass of atoms inside the superconductor. We used isotope species to change the mass of the atoms by a normal isotope effect [280–282]. There is no isotope effect when the non-electron-phonon mediator solely contributes the superconductivity [62]. One example is an $s^{\pm}$-wave superconductivity [62, 283–286]. The repulsive interband pair interaction (the positive interband Josephson interaction) is the origin of the $s^{\pm}$-wave superconductivity. This superconductivity is weakened under the attractive interband pair interaction (the negative interband Josephson interaction). There is competition between an $s^{\pm}$-wave and an s^{++}-wave, where the s^{++}-wave denotes the superconductivity in which the interband phase difference is zero radians. The inverse isotope effect occurs in this situation because the increase in the mass of the atoms weakens the interaction mediating the s^{++}-wave. Consequently, the strength of the disturbance against the interaction mediating the $s^{\pm}$-wave is suppressed, causing the enhancement of the $s^{\pm}$-wave. The T_c of the $s^{\pm}$-wave superconductivity increases as the mass of the element is increased. This is the inverse isotope effect. The isotope effect varies for different types of pnictide superconductors. This indicates the possibility that whether the s^{++}-wave or $s^{\pm}$-wave appears depends on the superconductor and the composition. The mechanism of the inverse isotope effect based on the competition of the s^{++}-wave and $s^{\pm}$-wave was well analyzed by Yanagisawa *et al* [287–289] and Choi *et al* [290].

The anomalous behavior discovered in the Meissner effect and heat capacity was suspected to be a consequence of the competition between the s^{++}-wave and $s^{\pm}$-wave. Tanaka, Shirage, and Iyo report that the Meissner effect and specific heat jump at T_c disappear in $(Ba_xK_{1-x})Fe_2As_2$ at $x = 0.2$ [291]. The tendency of the suppression of the specific heat jump was confirmed by the Loram group's precise measurement [292]. The weak Meissner effect suggests the presence of a strong pinning center that keeps the magnetic flux inside the sample. We cannot observe the diamagnetic signal by the Meissner

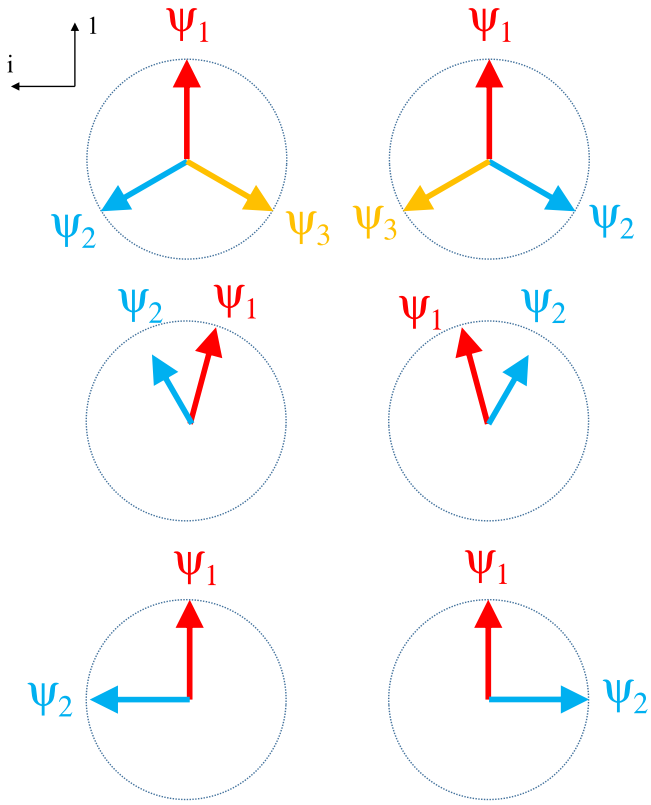

Figure 10. Arrangement of the order parameters of the chiral superconducting state. The upper panel shows the chiral state for a three-three component superconducting condensate. The middle panel shows the chiral state for a two-component frustrated superconducting condensate when an inter-component Josephson term is present. The lower panel shows the chiral state for a superconducting condensate composed of double degenerate components.

effect. However, the weak specific heat jump indicates that the superconductivity is weak, and a strong pinning force cannot be expected, because the pinning energy is primarily determined by the condensation energy of the superconductor [213]. These two experimental observations are inconsistent with each other. One plausible possibility to introduce the strong pinning center under a well-established superconducting condensate is the emergence of the domain structure, which was discussed in the p-wave triplet superconductivity by Sigrist and Agterberg [200]. This domain called a 'chiral domain'. As previously discussed, there are two degenerate superconducting states, denoted as $\Psi_1 + i\,\Psi_2$ and $\Psi_1 - i\,\Psi_2$. Each state becomes a domain, and the domain wall becomes a pinning center. When these two states emerge at T_c and mix, we have many domain walls acting as pinning centers. The domain structure assumes some portion of the entropies released by the formation of the pair, which suppress the specific heat jump at T_c because the jump is caused by the difference in the entropy between the normal state and superconducting state. The competition between the s^{++}-wave and $s^{\pm}$-wave gives rise to a new state with an interband phase difference whose absolute value is less than $\pi/2$, which can be denoted as $\Psi_1 + e^{i(\theta_2-\theta_1)}\,\Psi_2$, where θ_i is the phase of the ith component. This is illustrated in figure 10 along with other chiral states for comparison. This possibility is discussed by Tanaka, Shirage, and Iyo [293]. The biquadratic term between the two components is phenomenologically introduced to reproduce the competition between the s^{++}-wave and $s^{\pm}$-wave. Stanev and other researchers examined this scenario, including the microscopic origin, in detail [294, 295]. The domain structure was recently re-examined in detail by Garaud and Babaev [296]. In 1973, Lee proposed a similar situation known as the two-Higgs-doublet model [297], which is the simplest model to discuss the spontaneous time-reversal-symmetry violation in the field theory. However, the two-Higgs-doublet model does not include the quadratic cross term corresponding to the Josephson interaction.

Stanev and Tesanovic showed that the frustration due to the repulsive interaction in the three-band superconductor causes the broken time-reversal-symmetry-broken state [50]. It can be denoted as $\Psi_1 + e^{i(\theta_2-\theta_1)}\,\Psi_2 + e^{i(\theta_3-\theta_1)}\,\Psi_3$. Tanaka and Yanagisawa reached the same conclusion by the extension of their previous discussions on the frustration under the coexistence of the positive pair interaction and negative pair interaction [51, 202, 298]. The interband phase differences among three bands cannot become π simultaneously, because the sum of the three interband phase difference must be an integer multiple of 2π even when there are three positive interband interactions of which any two selected components tend to have the opposite sign. If three interband phase differences become π radians simultaneously, their sum becomes 3π. We can understand this more easily using the illustration of the arrangement of the component vector in the complex plane, as shown in figure 10. This is a basic mechanism for the emergence of the chiral superconductivity in a three-component superconductivity.

Before those discussions, there was discussion of the time-reversal-symmetry-broken state in the multiband superconductor. Agterberg *et al* mentioned the possibility of $\Psi_1 + e^{i(\theta_2-\theta_1)}\Psi_2$ [91]. They stated that the time-reversal-symmetry-broken state can be imagined by the combination of two non-degenerate components having the same symmetry. This was discussed for Sr_2RuO_4. They reported that the Leggett mode may grow into this state but did not mention the mechanism for this. Typically, the phase difference between two pairs should become zero because the intraband phase coherence is not achieved if a finite phase difference between two different parts occurs everywhere. This causes the destruction of the superconductivity. The zero phase difference between every two fragments in a Fermi surface is the basic criterion for the emergence of the usual superconductivity. We need a reason to align the phase in some sector and to form a finite phase difference between different sectors. The Leggett mode also needs a reason when it grows, becoming a static non-zero phase-difference mode. That is why this mechanism is actively discussed currently with regard to of the inter-component phase difference frustration. Agterberg also presented the time-reversal-symmetry breaking in the degenerate three-band superconductor in 1999 [49]. Wilson and Das stress that it is important to distinguish the time-reversal-symmetry breaking due to the frustration and

the degeneracy, because the time-reversal symmetry can be broken without the degeneracy [299]. This directly relates to the problem of the phase transition of the frustrated superconductivity without the degeneracy.

In an ordinary gap equation, the trial function is provided to keep the time-reversal symmetry. A gap parameter having both a real part and an imaginary part is included for the strong-coupling superconductor to express the real phonon emission [300]. This complex gap parameter describes the dissipation due to the emission of a real phonon. It may not be considered appropriate to describe the dissipation-less condition that we discuss here. It had stood to reason that the trial function, which can describe the time-reversal-symmetry-broken state, had not been examined well in the weak coupling theory. Tanaka and Yanagisawa mentioned the necessity to adopt the appropriate trial function including the time-reversal-symmetry-broken state for the BCS gap equation [298] even for the weak coupling theory with the non-dissipative situation. Stanev and Tesanovic also partially introduce the freedom into their trial function to discuss the time-reversal-symmetry-broken state [50]. The arbitrary interband phase difference and magnitude of the gap was examined comprehensively by Dias and Marques [301]. They discovered that the interband interaction should be very weak and stressed the role of the strong intraband interaction for the emergence of the time-reversal-symmetry-broken state. This is a very important finding. Stanev and Tesanovic considered that the time-reversal-symmetry-broken state can emerge without an intraband interaction. The strong intraband interaction was reported as a necessary condition in Tanaka and Yanagisawa's first work [51] because their discussion is an extension of the multicomponent superconductivity based on the multiband superconductor [21]. The picture of the superconducting condensate around the phase transition differs drastically depending on whether we adopt a weak interband interaction schema. In particular, it depends on the strength of the contrast between the intraband interaction and interband interaction.

According to Stanev and Tesanovic, the time-reversal-symmetry-broken state appears below T_c in the non-degenerated system, not at T_c [50]. The analysis of the BCS gap equation of Dian and Marques [301] and that of Wilson and Das support this statement [299]. The interband phase difference gradually grows at some temperature below T_c and approaches some value at a lower temperature. Mathematically, this tendency is due to the growth of the high-order terms, i.e., bi-quadratic terms or terms having order higher than 4 in the Ginzburg–Landau formalism [302]. Such terms retain the magnitude of the component, that is, they lock the magnitude so as not to be shrunk [51]. The system can determine the minimum energy by varying the interband phase difference. At T_c, there are only quadratic terms, which cannot lock the magnitude of the component. The system shrinks the magnitude of the component rather than varying the inter-component phase difference. On this view, the time-reversal-symmetry-broken state has no room to appear, and the interband phase difference becomes either 0 or π radians, as reported by Stanev and Tesanovic [50].

From the viewpoint of the spontaneous symmetry breaking [303, 304], the time-reversal-symmetry breaking seen in the chiral superconductivity needs some (continuous) symmetry to be broken. In a usual schema, this may be the rotational invariance of the inter-component phase difference. However, such symmetry has already been broken at T_c. The interband phase difference has been locked, and there is no rotational invariance. The system does not have any invariance to be sacrificed at the chiral transition (time-reversal-symmetry-broken transition). That is, the system does not retain any entropy realizing two different chiral states above the chiral transition.

From viewpoint of the double-order-parameter system, the second-order parameter is required [5]. In this case, the necessary entropy that will be lost at the chiral transition is introduced by the disorder state of the second-order parameter. Tesanovic and Stanev attributed the second-lowest solution of the BCS equation to this second-order parameter [50]. Unlike other multi-order-parameter systems, this system exhibits no disorder state of the second solution. Determining a source for the entropy required for the phase transition persists as a problem.

As Agterberg, Rice, and Sigrist discussed [91], the fluctuation above the chiral transition is an important issue to be examined. This fluctuation above the chiral transition temperature is some Leggett modes. Stanev proposed the mixed mode of the amplitude mode and phase difference mode as a seed of a chiral state [157]. Machida *et al* also suggested that the Leggett mode has a close relationship to the chiral state [305]. These discussions are based on the BCS formalism. However, we must be careful to examine the state near T_c and above the chiral transition temperature on the basis of the BCS formalism as mentioned before, because the entropy coming from the Leggett mode, which is the entropy of the pair, is dropped in the BCS gap equation [128]. When the pair has a certain entropy and a large Leggett mode fluctuation is present at T_c, the system may be treated as a multicomponent system. Alternatively, the system may be considered as a single-component superconductivity. These two views are not the same; recall them from the previous discussion of the type 1.5 superconductivity at T_c [113, 115].

The reduction in the energy of the Leggett mode observed in the frustrated superconductivity gives rise to the picture of the multicomponent superconductivity. It is apparent in the equivalent four-band case, where the four bands have the same density of states, the strength of the intraband interaction is the same for each band, and the interband interactions between any two bands are also the same. The massless Leggett mode appears and its emergence mechanism is very simple [46, 48]. Any relative phase between two groups gives the same Josephson energy when four components are divided into two groups having two members whose interband phase difference is π radians. This is illustrated in figure 5(e). In the three-band case, the reduction in the energy of the Leggett mode was noticeable [47], and it could be frozen at the chiral transition. There is a trick for this reduction that is not found in the Leggett mode

in the two-band superconductor. In the case of the two-band superconductor, the pure phase mode is not allowed, because we cannot make a circulation of the pair, as illustrated in figure 4(b), without the formation of the *i*-soliton, as previously discussed. However, we can make a pair circulation flow without changing the amplitude of the component in the Leggett mode of the frustrated three-component superconductivity [52], as illustrated in figure 4(c). This means that the excitation energy of the Leggett mode is scaled by the interband Josephson interaction, which is assumed to be very weak. The pair of the entropy should be considered in these systems.

Anishchanka, Volkov, and Efetov indicated the appearance of a massless mode in two-band superconductors near T_c for an un-frustrated system [306] in 2007. This corresponds to a second sound of the ^{4}He superfluid condensate, in which the superfluid component and normal component oscillate, anti-parallel to one another [254, 255, 258, 307–310]. In the ordinary superconductor, this is known as the Carlson–Goldman mode [311]. In the case of two-band superconductor, one component of the superconducting condensate can play the role of the normal component. The theoretical observation of the gapless (massless, or sound-like) nature of the Leggett mode suggests that the pair has a certain amount of entropy without the contribution of the normal component near T_c, which should be considered even in this system.

When we introduce the pair of the entropy into the BCS formalism, the gap tends not to close at mean field T_c [52]. It is owing to because the Leggett mode takes over some portion of the entropy of the fermion, after the fermion constitutes the pair and releases the entropy. According to the BCS gap equation, the cost due to the absence of the entropy caused by the pair formation should be compensated [128]. Then, the gap cannot open until the gain due to the opening of the superconducting gap can pay the cost. The formation of the gap becomes easier when the amount of missing entropy is reduced by the entropy inheritance due to the Leggett mode. The invariance of the interband phase difference rotation is restored by the large Leggett mode fluctuation, and it can give a pseudo-spontaneous symmetry breaking mechanism and supplies sufficient entropy at the chiral transition. Tanaka and Yanagisawa showed the interband phase locking transition on the basis of this scenario [312]. In this scenario, the order-parameter pattern varies according to the potential surface defined by the interband Josephson interaction in the phase space, as illustrated in figure 11. At higher temperatures, the fluctuation becomes large, and chiral states frequently convert into one another.

Unlike ordinary spontaneous symmetry-breaking phase transitions, this phase transition is of the first order. Stanev and Tesanovic also predicted the first-order transition about the chiral transition [50]. Experimentally, the multilayer cuprate superconductor, $HgBa_2Ca_4Cu_5O_y$, was discovered to exhibit the first-order phase transition below the superconducting transition temperature [313]. Because this system has five CuO_2 planes per unit cell, its superconducting state is considered to be in the multicomponent superconducting state. It is plausible that this phase transition is an example of the frustrated superconductivity discussed herein. Babaev *et al* presented a similar discussion of the interband phase difference unlocking state, considering only the entropy of the pairs and not that of the fermions [314]. They concluded that the interband phase difference unlocking state is a new non-superconducting state.

Regarding the interband phase difference unlocking state, we are aware of its similarity to the BEC-BCS crossover [315–321]. In the low-density fermion, the formation of the bound state of the fermion does not emerge from the superconductivity, even when the bound state is a boson. The overlapping of the wave function is small, and coherence does not appear. The system should be cooled to become a quantum condensate. This low density situation is the BEC limit. We can increase the density of the bound particles to achieve the coherence. The superconductivity appears after sufficient overlapping of the wave function; this indicates the BCS limit. In between, the mixing system of the boson and fermion is explored by tuning the strength of the binding energy in a cold fermion gas system [315]. In this discussion, there is only one characteristic length to specify the coherence. In the frustrated multicomponent superconductivity, there is an intraband coherence, but there is no coherence in the interband phase difference. The chiral transition is considered as the Leggett mode condensation. It is a type of the Bose condensation. There may be crossover between the Leggett mode condensates and the ordinary superconducting condensate in which the entropy of the pair is neglected [312].

Finally, we introduce the experimental realization of the time-reversal-symmetry-broken state due to the frustration. This was demonstrated by Sickinger *et al* [322]. This is an artificial two-component system realized using a so called π Josephson junction. The Josephson junction, in which the ferromagnetic metal is sandwiched by two superconductors, gives the π-radian phase shift between two superconducting layers when the thickness of the magnetic layer matches the half-period of oscillation of the amplitude of the superconducting order parameter inside the magnetic layer [323]. Here, the oscillation inside the magnetic layer is due to the finite momentum of the pair originating from the splitting of the spin up band and down band by the Zeeman effect. By varying the thickness of the magnetic layer, we can make both a π-Josephson junction and a 0-Josephson junction (0-Josephson denotes the normal Josephson junction giving zero phase difference between two superconducting sectors as the ground state). An $s^{\pm}$-wave appears in a π-Josephson junction, and an s^{++}-wave appears in a 0-Josephson junction, considering that this junction is a two-component system, as Moler did using the Al-bilayer system [42]. The competition between the $s^{\pm}$-wave and s^{++}-wave occurs when these two types of junctions are neighbors. As a result, the chiral state appears. This chiral state is the same as that discussed by Tanaka, Shirage, and Iyo [293]; Stanev and Koshelev [295]; and Maiti and A V Chubukov [294]. The critical current depends on which chiral state is selected and the direction of the current flow.

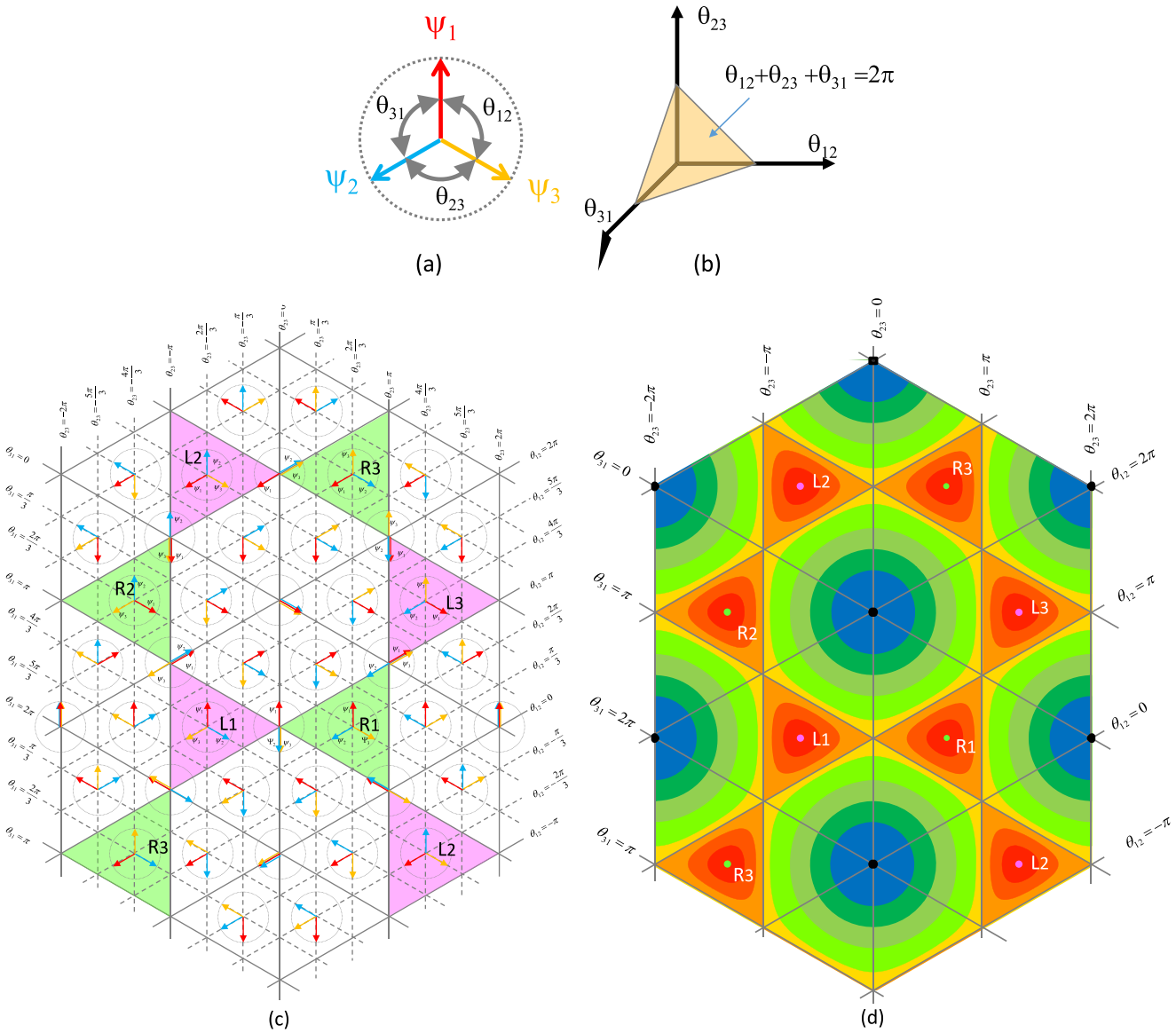

Figure 11. Potential contour map and order parameter arrangements of the three-component frustrated superconducting condensate, whose chiral situation is illustrated in the upper panel of figure 10. We show the definition of the coordinate of the inter-component relative phase in (a) and a constraint on them in (b). (c) The order parameter arrangement. In the colored area, we can make an internal pair circulation hopping. L_1, L_2, and L_3 have the same chirality. R_1, R_2, and R_3 also have the same chirality. Every pair selected from three members having the same chirality has a phase shift of either $2\pi/3$ or $-2\pi/3$. These pairs can be the next neighbor sandwiching a different chiral state. A phase variation can be read by connecting neighboring colored triangle centers. (d) A potential map of the inter-component Josephson interactions. The contours are −1.4, −1.2, −1.0, −0.8, 0.0, 1.0, and 2.0, which is normalized by the inter-component Josephson interaction constant. The potential bottom is at −1.5, and the top is at 3. The tops and bottoms are indicated by dots. The potential minima are denoted as L_i and R_i, using the same notation as (c).

The absolute value of the critical current of one direction of one chiral state is same as that of the reversed direction of another chiral state. Sickinger *et al* showed these two critical currents on their artificial three-component superconductor [322]. Two critical currents depending on the direction of the current flow was also shown for the junction composed of a single component superconductor and a three-band chiral superconductor theoretically by Huang and Hu [324]. Group of Jena University and IFW Dresden reported corresponding experimental indications [325, 326].

4. Summary

In this review, we introduce the definition and properties of the multicomponent superconductivity based on the multiband superconductor. The multicomponent superconductivity that emerges in the multiband superconductor depends on the contrast in the strength between the intraband pair interaction and the interband pair interaction. An ideal multicomponent superconductivity emerges when the interband interaction becomes very weak. Once multicomponent superconductivity emerges, topological objects such as the interband phase

difference soliton and the fractional vortices appear. These topological objects have common physics, which is discussed in the field theory, and other condensates such as the Bose–Einstein condensate of an atomic gas and superfluid ^{3}He. The multicomponent Ginzburg–Landau formalism, which is used to examine the properties of the multicomponent superconductivity based on the multiband superconductor, is widely used to study both dissipation-less and dissipative systems. The multicomponent superconductivity based on the multiband superconductor is a suitable and instructive model system for exploring the basic properties of the multicomponent system.

On the other hand, we cannot be always fully reliant on the Ginzburg–Landau formalism and the simple extension of the field theory. Such techniques cannot determine whether the system has a single component or multiple components at T_c. The first-order phase transition discussed in the frustration is also not covered. We must unify the field theory and the conventional superconducting paradigm to explore the statistical and thermodynamic properties of the multicomponent superconductivity based on the multiband superconductor. Bridging the microscopic theory and the Ginzburg–Landau formalism is one method for this unification. The contributions of the vital Leggett mode and pair entropy should be considered. The commonality among many exotic theories regarding the superconductor, which aim to surpass the BCS theory, is how to give an entropy to an object other than the fermion [327–332]. The multicomponent superconductivity based on the multiband superconductor may be the simplest mode including such an entropy. In this situation, the simple extension of the Gorkov method is no longer guaranteed [259]. We should determine whether there is a definite boundary between the multicomponent superconductivity based on multiband superconductors and the single-component superconductivity. There may be some crossover, such as the conventional BEC–BCS crossover.

The interband phase difference is a new gauge field that is electro-magnetically inactive as it is. It is very difficult to form a new neutral gauge field using the gauge field of the charged particle. However, it is a simple extension of the shielding of the twisted pair cable, as we use every day to reduce the electric noise. The realization of this technique in the field theory and superconducting circuits can lead to a new quantum Turing machine that is electromagnetically separated from the environment [17, 24]. The applications of the superconducting phase, including SQUIDs, remain very limited. We have the opportunity to discover new applications [333] using the interband phase difference.

Acknowledgments

The author thanks K Kikunaga (Kagoshima Univ.) for the original illustration of figure 8.

References

[1] Schawlow A L and Townes C H 1958 Infrared and optical masers *Phys. Rev.* **112** 1940–9
[2] Maiman T H 1960 Stimulated optical radiation in ruby *Nature* **187** 493–4
[3] Jaklevic R C, Lambe J, Mercereau J E and Silver A H 1965 Macroscopic quantum interference in superconductors *Phys. Rev.* **140** A1628–37
[4] Silver A H and Zimmerman J E 1967 Quantum states and transitions in weakly connected superconducting rings *Phys. Rev.* **157** 317–41
[5] Imry Y 1975 On the statistical mechanics of coupled order parameters *J. Phys. C: Solid State Phys.* **8** 567–77
[6] Sasaki S, Suganuma H and Toki H 1995 Dual Ginzburg–Landau theory with QCD-monopoles for dynamical chiral-symmetry breaking *Prog. Theor. Phys.* **94** 373–84
[7] Koma Y, Koma M, Ebert D and Toki H 2003 Effective string action for the U(1)xU(1) dual Ginzburg–Landau theory beyond the London limit *Nucl. Phys.* B **648** 189–202
[8] Nitta M, Eto M, Fujimori T and Ohashi K 2012 Baryonic bound state of vortices in multicomponent superconductors *J. Phys. Soc. Japan* **81** 084711
[9] Tanaka Y, Iyo A, Tokiwa K, Watanabe T, Crisan A, Sundaresan A and Terada N 2010 Topological structure of the inter-band phase difference soliton in two-band superconductivity *Physica* C **470** 1010–2
[10] Kibble T W D 1976 Topology of cosmic domains and strings *J. Phys. A: Math. Gen.* **9** 1387–98
[11] Pismen L M 1994 Energy versus topology: competing defect structures in 2D complex vector field *Phys. Rev. Lett.* **72** 2557–60
[12] Hoyuelos M and Jacobo A 2005 Characterization of phase singularities in the vector complex Ginzburg–Landau equation *Phys. Rev.* E **71** 017203
[13] Cross M C and Hohenberg P C 1993 Pattern formation outside of equilibrium *Rev. Mod. Phys.* **65** 851–1112
[14] Aranson I S and Pismen L M 2000 Interaction of vortices in a complex vector field and stability of a 'vortex molecule' *Phys. Rev. Lett.* **84** 634–7
[15] Montagne R and Hernández-García E 2000 Localized structures in coupled Ginzburg–Landau equations *Phys. Lett.* A **273** 239–44
[16] Hernandez-Garcia E, Hoyuelos M, Colet P and Miguel M S 1999 Spatiotemporal chaos, localized structure and synchronization in the vector complex Ginzburg–Landau equation *Int. J. Bifurcat. Chaos.* **9** 2257–64
[17] Tanaka Y, Iyo A, Terada N, Kawabata S, Sundaresan A, Watanabe T and Tokiwa K 2008 Quantum turing machine *United State Patent* 7,400,282 B2
[18] Yanagisawa T 2013 Quarks and fractionally quantized vortices in superconductors: an analogy between two worlds *Recent Advances in Quarks Research* ed H Fujikage and K Hyobanshi (New York: Nova Science) pp 113–46
[19] Yanagisawa T 2013 Theory of multi-band superconductivity *Recent Advances in Superconductivity Research* ed C B Taylor (New York: Nova Science) pp 219–48
[20] Tanaka Y 2001 Phase instability in multi-band superconductors *J. Phys. Soc. Japan* **70** 2844–7
[21] Tanaka Y 2002 Soliton in two-band superconductor *Phys. Rev. Lett.* **88** 017002
[22] Gurevich A and Vinokur V M 2003 Interband phase modes and nonequilibrium soliton structures in two-gap superconductors *Phys. Rev. Lett.* **90** 047004
[23] Cho Y M and Zhang P M 2008 Topological objects in two-gap superconductor *Eur. Phys. J.* B **65** 155–78
[24] Tanaka Y, Iyo A, Shivagan D D, Shirage P M, Tokiwa K, Watanabe T and Terada N 2010 Method for controlling

inter-component phase difference soliton and inter-component phase difference soliton circuit device *US Patent Application No* 2011/0063016
[25] Vakaryuk V, Stanev V, Lee W-C and Levchenko A 2012 Topological defect-phase soliton and the pairing symmetry of a two-band superconductor: role of the proximity effect *Phys. Rev. Lett.* **109** 227003
[26] Shen V L Y L, Senozan N M and Phillips N E 1965 Evidence for two energy gaps in high-purity superconducting Nb, Ta *Phys. Rev. Lett.* **14** 1025–7
[27] Gladstone G, Jensen M A and Schrieffer J R 1969 Superconductivity in the transition metals: theory and experiment *Superconductivity* ed R D Parks (New York: Dekker) sec. 13 pp 665–816
[28] Leggett A J 1966 Number-phase fluctuations in two-band superconductors *Prog. Theor. Phys.* **36** 901–30
[29] Mattheiss L F 1973 Band structure of transition-metal-dichalcogenide layer compounds *Phys. Rev.* B **8** 3719–40
[30] Koike Y, Suematsu H, Higuchi K and Tanuma S 1980 Superconductivity in graphite-alkali metal intercalation compounds *Physica* B+C **99** 503–8
[31] Hannay N B, Geballe T H, Matthias B T, Andres K, Schmidt P and MacNair D 1965 Superconductivity in graphitic compounds *Phys. Rev. Lett.* **14** 225–6
[32] Chevrel R, Prigent J and Sergent M 1971 Sur de nouvelles phases sulfurées ternaires du molybdène *J. Solid State Chem.* **3** 515–9
[33] Ihara K H, Tokiwa K, Ozawa H, hirabayashi M, Matsuhata H, Negishi A and Song Y S 1994 New high-T_c superconductor $Ag_{1-x}Cu_xBa_2Ca_{n-1}Cu_nO_{2n+3-\delta}$ family with $T_c > 117$ *Japan J. Appl. Phys.* **33** L300–3
[34] Hamada N and Ihara H 2001 Electronic band structure of $CuBa_2Ca_{n-1}Cu_nO2_{n+2}$ and $CuBa_2Ca_{n-1}Cu_nO_{2n+1}F$ (n = 3–5) *Physica* C **357–360** 108–11
[35] Tokunaga Y, Ishida K, Kitaoka Y, Asayama K, Tokiwa K, Iyo A and Ihara H 2000 Effect of carrier distribution on superconducting characteristics of the multilayered high-T_c cuprate $(Cu_{0.6}C_{0.4})Ba_2Ca_3Cu_4O_{12+y}$: ^{63}Cu–NMR study *Phys. Rev.* B **61** 9707–10
[36] Tanaka Y, Iyo A, Shirakawa N, Ariyama M, Tokumoto M, Ikeda S I and Ihara H 2001 Specific heat study on $Cu_xBa_2Ca_{n-1}Cu_nO_y$ *Physica* C **357–360** 222–5
[37] Crisan A, Tanaka Y, Shivagan D D, Iyo A, Cosereanu L, Tokiwa K and Watanabe T J 2007 Anomalous AC susceptibility response of $(Cu,C)Ba_2Ca_2Cu_3O_y$: experimental indication of two-component vortex matter in multi-layered cuprate superconductors *Appl. Phys.* **46** L451–3
[38] Tanaka Y, Crisan A, Shivagan D D, Iyo A, Tokiwa K and Watanabe T 2007 Interpretation of abnormal AC loss peak based on vortex-molecule model for a multicomponent cuprate superconductor *Japan J. Appl. Phys.* **46** 134–45
[39] Shivagan D D, Crisan A, Shirage P M, Sundaresan A, Tanaka Y, Iyo A, Tokiwa K, Watanabe T and Terada N 2009 Vortex molecule and i-soliton studies in multilayer cuprate superconductors *J. Phys.: Conf. Ser.* **97** 012212
[40] Nagamatsu J, Nakagawa N, Muranaka T, Zenitani Y and Akimitsu J 2001 Superconductivity at 39 K in magnesium diboride *Nature* **410** 63–4
[41] Kamihara Y, Hiramatsu H, Hirano M, Kawamura R, Yanagi H, Kamiya T and Hosono H 2006 Iron-based layered superconductor: LaOFeP *J. Am. Chem. Soc.* **128** 10012–3
[42] Bluhm H, Koshnick N C, Huber M E and Moler K A 2006 Magnetic response of mesoscopic superconducting rings with two order parameters *Phys. Rev. Lett.* **97** 237002
Bluhm H, Koshnick N C, Huber M E and Moler K A 2007 *Phys. Rev. Lett.* **98** 209902(E) (erratum)
[43] Guikema J W, Bluhm H, Bonn D A, Liang R, Hardy W N and Moler K A 2008 Two-dimensional vortex behavior in highly underdoped $YBa_2Cu_3O_{6+x}$ observed by scanning Hall probe microscopy *Phys. Rev.* B **77** 104515
[44] Luan L, Auslaender O M, Bonn D A, Liang R, Hardy W N and Moler K A 2009 Magnetic force microscopy study of interlayer kinks in individual vortices in the underdoped cuprate superconductor $YBa_2Cu_3O_{6+x}$ *Phys. Rev.* B **79** 214530
[45] Babaev E 2002 Vortices with fractional flux in two-gap superconductors and in extended Faddeev model *Phys. Rev. Lett.* **89** 067001
[46] Tanaka Y, Yanagisawa T, Crisan A, Shirage P M, Iyo A, Tokiwa K, Nishio T, Sundaresan A and Terada N 2011 Domains in multiband superconductors *Physica* C **471** 747–50
[47] Lin S-Z and Hu X 2012 Massless leggett mode in three-band superconductors with time-reversal-symmetry breaking *Phys. Rev. Lett.* **108** 177005
[48] Yanagisawa T and Hase I J 2013 Massless modes and abelian gauge fields in multi-band superconductors *Phys. Soc. Japan* **82** 124704
[49] Agterberg D F, Barzykin V and Gor'kov L P 1999 Conventional mechanisms for exotic superconductivity *Phys. Rev.* B **60** 14868–71
[50] Stanev V and Tesanovic Z 2010 Three-band superconductivity and the order parameter that breaks time-reversal symmetry *Phys. Rev.* B **81** 134522
[51] Tanaka Y and Yanagisawa T 2010 Chiral ground state in three-band superconductors *J. Phys. Soc. Japan* **79** 114706
[52] Tanaka Y, Yanagisawa T and Nishio T 2012 Fluctuation-assisted gap evolution in frustrated multiband superconductors *Physica* C **483** 86–90
[53] Moshchalkov V, Menghini M, Nishio T, Chen Q H, Silhanek A V, Dao V H, Chibotaru L F, Zhigadlo N D and Karpinski J 2009 Type-1.5 superconductivity *Phys. Rev. Lett.* **102** 117001
[54] Babaev E and Speight M 2005 Semi-Meissner state and neither type-I nor type-II superconductivity in multicomponent superconductors *Phys. Rev.* B **72** 180502(R)
[55] Anderson M H, Ensher J R, Matthews M R, Wieman C E and Cornell E A 1995 Observation of Bose–Einstein condensation in a dilute atomic vapor *Science* **269** 198–201
[56] Matthews M R, Anderson B P, Haljan P C, Wieman C E and Cornell E A 1999 Vortices in a Bose–Einstein condensate *Phys. Rev. Lett.* **83** 2498–501
[57] Osheroff D D, Richardson R C and Lee D M 1972 Evidence for a new phase of solid ^{3}He *Phys. Rev. Lett.* **28** 885–8
[58] Leggett A J 1972 Interpretation of recent results on He^3 below 3 mK: a new liquid phase? **29** 1227–30
[59] Leggett A J 1975 A theoretical description of the new phases of liquid ^{3}He *Rev. Mod. Phys.* **47** 331–414
[60] Bardeen J, Cooper L N and Schrieffer J R 1957 Theory of superconductivity *Phys. Rev.* **108** 1175–204
[61] Suhl H, Matthias B T and Walker L R 1959 Bardeen–Cooper–Schrieffer theory of superconductivity in the case of overlapping bands *Phys. Rev. Lett.* **3** 552
[62] Kondo J 1963 Superconductivity in transition metals *Prog. Theor. Phys.* **29** 1–9
[63] Peretti J 1962 Superconductivity of transition elements *Phys. Lett.* **2** 275–6
[64] Babaev E, Faddeev L D and Niemi A J 2002 Hidden symmetry and knot solitons in a charged two-condensate Bose system *Phys. Rev.* B **65** 100512(R)
[65] Cho Y M and Zhang P 2006 Non-Abrikosov vortex and topological knot in two-gap superconductors *Phys. Rev.* B **73** 180506(R)
[66] Eto M, Hirono Y, Nitta M and Yasui S 2014 Vortices and other topological solitons in dense quark matter *Prog. Theor. Exp. Phys.* **2014** 012D01

[67] Ivanov I P 2009 General two-order-parameter Ginzburg–Landau model with quadratic and quartic interactions *Phys. Rev.* E **79** 021116

[68] Yerin Y S and Omelyanchouk A N 2007 Coherent current states in a two-band superconductor *Low Temp. Phys.* **33** 401–7

[69] Doria M M, Romaguera A R de C and Peeters F M 2010 The ground states of the two-component order paramater superconductor *Eur. Phys. Lett.* **92** 17004

[70] Xi X X 2008 Two-band superconductor magnesium diboride *Rep. Prog. Phys.* **71** 116501

[71] Geilikman B T and Kresin V Z 1963 Effect of anisotropy on the properties of superconductors *Fiz. Tverd. Tela* **5** 3549–59
Geilikman B T and Kresin V Z 1964 *Sov. Phys.-Solid State* **5** 2605–11

[72] Bennett A J 1965 Theory of the anisotropic energy gap in superconducting lead *Phys. Rev.* **140** A1902–20

[73] Sanna A, Profeta G, Floris A, Marini A, Gross E K U and Massidda S 2007 Anisotropic gap of superconducting CaC_6: a first-principles density functional calculation *Phys. Rev.* B **75** 020511(R)

[74] Bouquet F, Fisher R A, Phillips N E, Hinks D G and Jorgensen J D 2001 Specific heat of $Mg^{11}B_2$: evidence for a second energy gap *Phys. Rev. Lett.* **87** 047001

[75] Bouquet F, Wang Y, Fisher R A, Hinks D G, Jorgensen J D, Junod A and Phillips N E 2001 Phenomenological two-gap model for the specific heat of MgB_2 *Europhys. Lett.* **56** 856–62

[76] Nakajima Y, Nakagawa T, Tamegai T and Harima H 2008 Specific-heat evidence for two-gap superconductivity in the ternary-iron silicide $Lu_2Fe_3Si_5$ *Phys. Rev. Lett.* **100** 157001

[77] Mishonov T and Penev E 2002 Thermodynamics of anistropic-gap and multi-band clean BCS superconductors *Int. J. Mod. Phys.* B **16** 3573–3568

[78] Haas S and Maki K 2001 Anisotropic s-wave superconductivity in MgB_2 *Phys. Rev.* B **65** 020502(R)

[79] Mishonov T M, Penev E S and Indekeu J O 2002 Comment on anistropic s-wave superconductivity in MgB_2 *Phys. Rev.* B **66** 066501

[80] Bersier C *et al* 2009 Multiband superconductivity in Pb, H under pressure and CaBeSi from ab initio calculations *J. Phys.: Condens. Matter* **21** 164209

[81] Floris A, Sanna A, Massidda S and Gross E K U 2007 Two-band superconductivity in Pb from ab initio calculations *Phys. Rev.* B **75** 054508

[82] Choi H J, Roundy D, Sun H and Cohen M L 2002 The origin of the anomalous superconducting properties of MgB_2 *Nature* **418** 758–60

[83] Margine E R and Giustino F 2013 Anisotropic Migdal–Eliashberg theory using wannier functions *Phys. Rev.* B **87** 024505

[84] Konsin P and Sorkin B 2004 A generalized two-band model for the superconductivity in MgB_2 *Supercond. Sci. Technol.* **17** 1472–6

[85] Vargunin A, Örd T and Rägo Supercond K J 2011 Thermal fluctuations of order parameters in two-gap superconductors *Nov. Magn.* **24** 1127–31

[86] Vargunin A, Rägo K and Örd T 2013 Two-gap superconductivity: interband interaction in the role of an external field *Supercond. Sci. Technol.* **26** 065008

[87] Khasanov R, Bendele M, Amato A, Konder K, Keller H, H-Klauss H, Luetkens H and Pomjakushina E 2010 Evolution of two-gap behavior of the superconductor $FeSe_{1-x}$ *Phys. Rev. Lett.* **104** 087004

[88] Maksimov E G, Karakozov A E, Gorshunov B P, Zhukova E S, Ya Ponomarev G and Dressel M 2011 Electronic specific heat of two-band layered superconductors: analysis within the generalized two-band α model *Phys. Rev.* B **84** 174504

[89] Zhitomirsky M E and Rice T M 2001 Interband proximity effect and nodes of superconducting Gap in Sr_2RuO_4 *Phys. Rev. Lett.* **87** 057001

[90] Kogan V G, Martin C and Prozorov R 2009 Superfluid density and specific heat within a self-consistent scheme for a two-band superconductor *Phys. Rev.* B **80** 014507

[91] Agterberg D F, Rice T M and Sigrist M 1997 Orbital dependent superconductivity in Sr_2RuO_4 *Phys. Rev. Lett.* **78** 3374–7

[92] Golubov A A and Koshelev A E 2003 Upper critical field in dirty two-band superconductors: breakdown of the anisotropic Ginzburg–Landau theory *Phys. Rev.* B **68** 104503

[93] Shanenko A A, Milošević M V, Peeters F M and Vagov A V 2011 Extended Ginzburg–Landau formalism for two-band superconductors *Phys. Rev. Lett.* **106** 047005

[94] Vagov A, Shanenko A A, Milošević M V, Axt V M and Peeters F M 2012 Two-band superconductors: extended Ginzburg–Landau formalism by a systematic expansion in small deviation from the critical temperature *Phys. Rev.* B **86** 144514

[95] MacVicar M L A and Rose R M 1968 Anisotropic energy-gap measurements on duperconducting niobium single crystals by tunneling *J. Appl. Phys.* **39** 1721–7

[96] Sung C C and Wong V K 1967 Influence of nonmagnetic impurities on superconductors with overlapping bands *J. Phys. Chem. Solids* **28** 1933–40

[97] Bostock J, Agyeman K, Frommer M H and MacVicar M L A 1973 Determining accurate superconducting tunneling energy gaps: anisotropy in single crystal Nb *J. Appl. Phys.* **44** 5567–9

[98] Golubov A A and Mazin I I 1997 Effect of magnetic and nonmagnetic impurities on highly anisotropic superconductivity *Phys. Rev.* B **55** 15146–52

[99] Annett J F, Goldenfeld N and Leggett A J 1996 Experimental constrains on the paring state of the cuprate superconductors: an emergening consensus *Physical Properties of High Temperature Superconductors V.* ed D M Ginsberg (Singapore: World Scientific) pp 375–461

[100] Abrikosov A A 1957 On the magnetic properties of superconductors of the second group *Sov. Phys. JETP* **5** 1174–83

[101] Faber T E 1958 The Intermediate state in superconducting plates *Proc. R. Soc.* A **248** 460–81

[102] Biagi K R, Kogan V G and Clem J R 1985 Perpendicular upper critical field of superconducting–normal-metal multilayers *Phys. Rev.* B **32** 7165–72

[103] Takahashi S and Tachiki M 1986 Theory of the upper critical field of superconducting superlattices *Phys. Rev.* B **33** 4620–31

[104] Gurevich A 2003 Enhancement of the upper critical field by nonmagnetic impurities in dirty two-gap superconductors *Phys. Rev.* B **67** 184515

[105] Nishio T, Dao V H, Chen Q, Chibotaru L F, Kadowaki K and Moshchalkov V V Scanning SQUID microscopy of vortex clusters in multiband superconductors 2010 *Phys. Rev.* B **81** 020506(R)

[106] Bean C P 1962 Magnetization of hard superconductors *Phys. Rev. Lett.* **8** 250–3

[107] Bitter F 1931 On inhomogeneities in the magnetization of ferromagnetic materials *Phys. Rev.* **38** 1903–5

[108] Bitter F 1932 Experiments on the nature of ferromagnetism *Phys. Rev.* **41** 507–15

[109] Essmann U and Träuble H 1967 The direct observation of individual flux lines in type II superconductors *Phys. Lett.* A **24** 526–7

[110] Morooka T, Nakayama S, Odawara A, Ikeda M, Tanaka S and Chinone K 1999 Micro-imaging system using scanning DC-SQUID microscope *IEEE Trans. Appl. Supercond.* **9** 3491–4

[111] Geyer J, Fernandes R M, Kogan V G and Schmalian J 2010 Interface energy of two-band superconductors *Phys. Rev.* B **82** 104521

[112] Kogan V G and Schmalian J 2011 Ginzburg–Landau theory of two-band superconductors: absence of type-1.5 superconductivity *Phys. Rev.* B **83** 054515

[113] Kogan V G and Schmalian J 2012 Reply to 'comment on 'Ginzburg–Landau theory of two-band superconductors: absence of type-1.5 superconductivity' *Phys. Rev.* B **86** 016502

[114] Silaev M and Babaev E 2011 Microscopic theory of type-1.5 superconductivity in multiband systems *Phys. Rev.* B **84** 094515

[115] Babaev E and Silaev M 2012 Comment on 'Ginzburg–Landau theory of two-band superconductors: absence of type-1.5 superconductivity' *Phys. Rev.* B **86** 016501

[116] Babaev E, Carlström J, Garaud J, Silaev M and Speight J M 2012 Type-1.5 superconductivity in multiband systems: magnetic response, broken symmetries and microsciopic theory–a brief overview *Physica* C **479** 2–14

[117] Carlström J, Garaud J and Babaev E 2011 Length scales, collective modes, ant type-1.5 regimes in three-band superconductors *Phys. Rev.* B **84** 134518

[118] Ichioka M, Hayashi N, Enomoto N and Machida K 1995 Fundamental properties of a vortex in a d-wave superconductor *J. Phys. Soc. Japan* **64** 4547–51

[119] Ichioka M, Hayashi N, Enomoto N and Machida K 1996 Vortex structure in d-wave superconductors *Phys. Rev.* B **53** 15316–26

[120] Ichioka M, Enomoto N, Hayashi N and Machida K 1996 s- and dxy-Wave components induced around a vortex in dx^2-y^2-wave superconductors *Phys. Rev.* B **53** 2233–6

[121] Franz M, Kallin C, Soinien P I, Berlinsky A J and Fetter A L 1996 Vortex state in a d-wave superconductor *Phys. Rev.* B **53** 5795–814

[122] Ren Y, Xu J-H and Ting C S 1995 Ginzburg–Landau equations and vortex structure of a dx^2-y^2 superconductor *Phys. Rev. Lett.* **74** 3680–3

[123] Xu J-H, Ren Y and Ting C S 1995 Ginzburg–Landau equationis for a d-wave superconductor with application to vortex structure and surface problems *Phys. Rev.* B **52** 7663–74

[124] Berlinsky A J, Fetter A L, Franz M, Kallin C and Soininen P I 1995 Ginzburg–Landau theory of vortices in d-wave superconductors *Phys. Rev. Lett.* **75** 2200–3

[125] Hu X and Wang Z 2012 Stability and Josephson effect of time-reversal-symmetry-broken multicomponent superconductivity induced by frustrated intercomponent coupling *Phys. Rev.* B **85** 064516

[126] Ivanov I P and Vdgovin E 2012 Discrete symmetries in the three-Higgs-doublet model *Phys. Rev.* D **86** 095030

[127] Romaguera A R, de C and Silva K J S 2013 Variational method applied to two-component Ginzburg–Landau theory *J. Math. Phys.* **54** 093501

[128] Bardeen J and Schrieffer J R 1961 Recent developments in superconductivity *Prog. Low Temp. Phys.* **3** 170–287

[129] Anderson P W 1958 Random-phase approximation in the theory of superconductivity *Phys. Rev.* **112** 1900–16

[130] Tachiki M, Koyama T and Takahashi S 1994 Electromagnetic phenomena related to a low-frequency plasma in cuprate superconductors *Phys. Rev.* B **50** 7065–84

[131] Rickayzen G 1959 Collective excitations in the theory of superconductivity *Phys. Rev.* **115** 795–808

[132] Tsuneto T 1960 Transverse collective excitations in superconductors and electromagnetic absorption *Phys. Rev.* **118** 1029–35

[133] Littlewood P B and Varma C M 1982 Amplitude collective modes in superconductors and their coupling to charge-density waves *Phys. Rev.* B **26** 4883–93

[134] Sooryakumar R and Klein M V 1980 Raman scattering by superconducting-gap exicitations and their coupling to charge-density wave *Phys. Rev. Lett.* **45** 660–2

[135] Matsunaga R and Shimano R 2012 Nonequilibrium BCS state dynamics induced by intense terahertz pulses in a superconducting NbN film *Phys. Rev. Lett.* **109** 187002

[136] Matsunaga R, Tsuji N, Fujita H, Sugino A, Makisem K, Uzawa Y, Terai H, Wang Z, Aoki H and Shimano R 2014 Light-induced collective pseudospin precession resonating with Higgs mode in a superconductor *Science* **345** 1145–9

[137] Izyumov Y A and Laptev V M 1990 Vortex structure in superconductors with a many component order parameter *Phase Transit.* **20** 95–112

[138] Wu W-C and Griffin A 1995 Phase and amplitude modes in a superconductor with interlayer pair tunneling *Phys. Rev. Lett.* **74** 158–61

[139] Kon L Z, Ciobanu I P and Digor D F 1997 Raman scattering in two-band superconductors *J. Phys.: Condens. Matter* **9** 3821

[140] Kochorbé F G and Palistrant M E J 1998 Collective oscillations in two-band superconducting systems with low carrier density *Exp. Theor. Phys.* **87** 570–80

[141] Hadjiev V G, Zhou X, Strohm T, Cardona M, Lin Q M and Chu C W 1998 Strong superconductivity-induced phonon self-energy effects in $HgBa_2Ca_3Cu_4O_{10+\delta}$ *Phys. Rev.* B **58** 1043–50

[142] Hadjiev V G, Martin A A, Ruf T and Cardona M 1999 Phonon self-energy effects in high-temperature superconductors *Phys. Status Solidi* b **215** 483–8

[143] Limonov M, Lee S, Tajima S and Yamanaka A 2002 Superconductivity-induced resonant Raman scattering in multilayer high-T_c superconductors *Phys. Rev.* B **66** 054509

[144] Tanaka Y, Iyo A, Kato H, Tokiwa K, Watanabe T and Ihara H 2002 The role of multiple gaps on the Raman spectrum of $(Cu_xC_{1-x})Ba_2Ca_{n-1}CunOy$ *Physica* C **378–381** 283–6

[145] Tanaka Y, Iyo A, Takahashi S, Hirai M, Okumoto H, Kato H, Tokiwa K and Watanabe T 2003 Dynamics of multiple order parameters in the multi-band superconductor studied by Raman spectroscopy *Physica* C **392–396** 161–5

[146] Blumberg G, Mialitsin A B, Dennis S, Klein M V, Zhigadlo N D and Karpinski J 2007 Observation of Leggett's collective mode in a multiband MgB_2 superconductor *Phys. Rev. Lett.* **99** 227002

[147] Blumberg G, Mialitsin A, Dennis B S, Zhigadlo N D and Karpinski J 2007 Multi-gap superconductivity in MgB_2: magneto-Raman spectroscopy *Physica* C **456** 75–82

[148] Klein M V 2010 Theory of Raman scattering from Leggett's collective mode in a multiband superconductor: application to MgB_2 *Phys. Rev.* B **82** 014507

[149] Chubukov A V, Eremin I and Korshunov M M 2009 Theory of Raman response of a superconductor with extended s-wave symmetry: application to the iron pnictides *Phys. Rev.* B **79** 220501(R)

[150] Ponomarev Y G *et al* 2004 Evidence for a two-band behavior of MgB_2 from point-contact and tunneling spectroscopy *Solid State Commun.* **129** 85–9

[151] Agterberg D F, Demler E and Janko B 2002 Josephson effects between multigap and single-gap superconductors *Phys. Rev.* B **66** 214507

[152] Ota Y, Machida M, Koyama T and Matsumoto H 2009 Theory of heterotic superconductor-insulator-superconductor Josephson junctions between single- and multiple-gap superconductors *Phys. Rev. Lett.* **102** 237003

[153] Asai H, Ota Y, Kawabata S, Machida M and Nori F 2014 Theory of macroscopic quantum tunneling with Josephson–Leggett collective excitations in multiband superconducting Josephson junctions *Phys. Rev.* B **89** 224507

[154] Ng T K and Nagaosa N 2009 Broken time-reversal symmetry in Josephson junction involving two-band superconductors *Eur. Phys. Lett.* **87** 17003

[155] Koshelev A E and Stanev V 2011 Proximity fingerprint of s ±-superconductivity *Eur. Phys. Lett.* **96** 27014

[156] Bobkov A M and Bobkova I V 2011 Time-reversal symmetry breaking state near the surface of an s± superconductor *Phys. Rev.* B **84** 134527

[157] Stanev V 2012 Model of collective modes in three-band superconductors with repulsive interband interactions *Phys. Rev.* B **85** 174520

[158] Marciani M, Fanfarillo L, Castellani C and Benfatto L 2013 Leggett modes in iron-based superconductors as a probe of time-reversal symmetry breaking *Phys. Rev.* B **88** 214508

[159] Kobayashi K, Ota Y and Machinda M 2013 Analysis of collective excitation for multi band superconductor: frustrated spin model approach *Physica* C **494** 13–6

[160] Kobayashi K, Machida M, Ota Y and Nori F 2013 Massless collective excitations in frustrated multiband superconductors *Phys. Rev.* B **88** 224516

[161] Skyrme T H R 1959 A unified model of K- and π mesons *Proc. R. Soc.* A **252** 236–45

[162] Finkelstein D 1966 Kinks *J. Math. Phys.* **7** 1218–25

[163] Bloch F 1932 Zur theorie des austauschproblems und der remanenzerscheinung der ferromagnetika *Z. Phys.* **74** 295–335

[164] Maki K and Tsuneto T 1975 Magnetic resonance and spin waves in the a phase of superfluid ^{3}He *Phys. Rev.* B **11** 2539–43

[165] Maki K and Ebisawa H 1976 Magnetic excitations in superfluid ^{3}He *J. Low Temp. Phys.* **23** 351–65

[166] Tokuyasu T A, Hess D W and Sauls J A 1990 Vortex states in an unconventional superconductor and the mixed phases of UPt_3 *Phys. Rev.* B **41** 8891–903

[167] Son D T and Stephanov M A 2002 Domain walls of relative phase in two-component Bose–Einstein condensates *Phys. Rev.* A **65** 063621

[168] Rabi I I 1937 Space quantization in a gyrating magnetic field *Phys. Rev.* **51** 652–4

[169] Loudon R 1983 *The Quamtum Theory of Light* 2nd edn (Oxford: Clarendon) Section 2

[170] Crisan A, Tanaka Y, Iyo A, Cosereanu L, Tokiwa K and Watanabe T 2006 Anomalous vortex melting line in the two-component superconductor (Cu,C)$Ba_2Ca_3Cu_4O_{10+\delta}$ *Phys. Rev.* B **74** 184517

[171] Ogino M, Watanabe T, Tokiwa K, Iyo A and Ihara H 1996 Hall effect of superconducting copper oxide, Cu-1234 *Physica* C **258** 384–8

[172] Hirai M, Iyo A, Kodama Y, Sundaresan A, Arai J and Tanaka Y 2004 Anomalous behaviour of irreversibility lines in multi-layered superconductor (Cu,C)$Ba_2Ca_3Cu_4O_y$ *Supercond. Sci. Technol.* **17** 423–9

[173] Tanaka Y 2003 The final report of *The Creation of the Best Performance Superconductor* sponsored by Strategic Basic Research Programs (CREST) of Japan Science and Technology Agency p 39 figure 35 (in Japanese) (available at www.jst.go.jp/kisoken/crest/report/sh_heisei10/denshikoushi/tanaka.pdf)

[174] Žutić I, Fabian J and Sarma D S 2004 Spintronics: fundamentals and applications *Rev. Mod. Phys.* **76** 323–410

[175] Scott A C 1969 A nonlinear Klein–Gordon equation *Am. J. Phys.* **37** 52–61

[176] Salerno M and Scott A C 1982 Linewidth for fluxon oscillators *Phys. Rev.* B **26** 2474–81

[177] Kondo Y, Korhonen J S, Krusius M, Dmitriev V V, Thuneberg E V and Volovik G E 1992 Combined spin-mass vortex with soliton tail in superfluid ^{3}He-B *Phys. Rev. Lett.* **68** 3331–4

[178] Fulton T A and Dynes R C 1973 Single vortex propagation in Josephson tunneling junction *Solid State Commun.* **12** 57–61

[179] Akoh H, Sakai S and Takada S 1987 Direct observation of fluxon reflection in a Josephson transmission line *Phys. Rev.* B **35** 5357–60

[180] Nakajima K, Mizusawa H, Sawada Y, Akoh H and Takadam S 1990 Experimental observation of spatiotemporal wave forms of all possible types of soliton-antisoliton interactions in Josephson transmission lines *Phys. Rev. Lett.* **65** 1667–70

[181] Gurevich A and Vinokur V M 2006 Phase textures induced by dc-current pair breaking in weakly coupled multilayer structures and two-gap superconductors *Phys. Rev. Lett.* **97** 137003

[182] Kopelevich Y, Ciovacco F, Esquinazi P and Lorenz M 1998 Nonlocal in-plane resistance due to vortex-antivortex dynamics in high-T_c superconducting films *Phys. Rev. Lett.* **80** 4048

[183] Miu L, Jakob G and Adrian H 1999 Comment on nonlocal in-plane resistance due to vortex-antivortex dynamics in high-T_c superconducting films *Phys. Rev. Lett.* **82** 672

[184] Miu L, Jakob G, Adrian Kopelevich H Y and Esquinazi P 1999 A reply to the comment *Phys. Rev. Lett.* **82** 673

[185] Mrowka F, Manzoor S, Pongpiyapaiboon P, Maksimov I L, Esquinazi P, Zimmer K and Lorenz M 2003 Excess voltage in the vicinity of the superconducting transition in inhomogeneous $YBa_2Cu_3O_7$ thin films *Physica* C **399** 22–42

[186] Octavio M, Skocpol W J and Tinkham M 1978 Nonequilibrium-enhanced supercurrents in short superconducting weak links *Phys. Rev.* B **17** 159–69

[187] Yerin Y S and Omelyanchouk A N 2010 Josephson currents in point contacts between dirty two-band superconductors *Low Temp. Phys.* **36** 969–73

[188] Yerin Y S, Fenchenko V N and Il'ichev E V 2013 Phase diagram of the resistive state of a narrow superconducting channel in the voltage-driven regime *Low Temp. Phys.* **39** 125–32

[189] Fenchenko V N and Yerin Y S 2012 Phase slip centers in a two-band superconducting filament: application to MgB_2 *Physica* C **480** 120–36

[190] Yerin Y S and Fenchenko V N 2013 Dynamics of the resistive state of a narrow superconducting channel in the ac voltage driven regime *Low Temp. Phys.* **39** 1023–31

[191] Kogan V G 1981 London approach to anisotropic type-II superconductors *Phys. Rev.* B **24** 1572–5

[192] Little W A and Parks R D 1962 Observation of quantum periodicity in the transition temperature of a superconducting cylinder *Phys. Rev. Lett.* **9** 9–12

[193] Parks R D and Little W A 1964 Fluxoid quantization in a multiply-connected superconductor *Phys. Rev.* **133** A97–103

[194] Erin Y S, Kuplevakhskiĭ S V and Omel'yanchuk A N 2008 Little–Parks effect for two-band superconductors *Low Temp. Phys.* **34** 891–7

[195] Koshnick N C, Bluhm H, Huber M E and Moler K A 2007 Fluctuation superconductivity in mesoscopic aluminum rings *Science* **318** 1440–3

[196] Kuplevakhsky S V, Omelyanchouk A N and Yerin Y S 2011 Soliton states in mesoscopic two-band-superconducting cylinders *Low Temp. Phys.* **37** 667–77

[197] Samokhin K V 2012 Phase solitons and subgap excitations in two-band superconductors *Phys. Rev.* B **86** 064513

[198] Tsuei C C, Kirtley J R, Ren Z F, Wang J H, Raffy H and Li Z Z 1997 Pure dx^2–y^2 order-parameter symmetry in the tetragonal superconductor $Tl_2Ba_2CuO_{6+\delta}$ *Nature* **387** 481–3

[199] Tsuei C C, Kirtley J R, Chi C C, Yu-Jahnes L S, Gupta A, Shaw T, Sun J Z and Ketchen M B 1994 Pairing symmetry and flux quantization in a tricrystal superconducting ring of $YBa_2Cu_3O_{7-\delta}$ *Phys. Rev. Lett.* **73** 593–6

[200] Sigrist M and Agterberg D F 1999 The role of domain walls on the vortex creep dynamics in unconventional superconductors *Prog. Theor. Phys.* **102** 965–81

[201] Jang J, Ferguson D G, Vakaryuk V, Budakian R, Chung S B, Goldbart P M and Maeno Y 2011 Observation of half-height magnetization steps in Sr_2RuO_4 *Science* **331** 186–8

[202] Yanagisawa T, Tanaka Y, Hase I and Yamaji K 2012 Vortices and chirality in multi-band superconductors *J Phys. Soc. Japan* **81** 024712

[203] Garaud J, Carlström J and Babaev E 2011 Topological solitons in three-band superconductors with broken time reversal symmetry *Phys. Rev. Lett.* **107** 197001

[204] Lin S-Z and Hu X 2012 Phase solitons in multi-band superconductors with and without time-reversal symmetry *New J. Phys.* **14** 063021

[205] Chibotaru L F and Dao V H 2010 Stable fractional flux vortices in mesoscopic superconductors *Phys. Rev.* B **81** 020502(R)

[206] Chibotaru L F, Dao V H and Ceulemans A 2007 Thermodynamically stable noncomposite vortices in mesoscopic two-gap superconductors *Eur. Phys. Lett.* **78** 47001

[207] Gillis S, Jäykkä J and Milošević M V 2014 Vortex states in mesoscopic three-band superconductors *Phys. Rev.* B **89** 024512

[208] Geurts R, Milošević M V, Aguiar J A and Peeters F M 2013 Enhanced stability of vortex-antivortex states in two-component mesoscopic superconductors *Phys. Rev.* B **87** 024501

[209] Geurts R, Milošević M V and Peeters F M 2010 Vortex matter in mesoscopic two-gap superconducting disks: influence of Josephson and magnetic coupling *Phys. Rev.* B **81** 214514

[210] Pereira P J, Chibotaru L F and Moshchalkov V V 2011 Vortex matter in mesoscopic two-gap superconductor square *Phys. Rev.* B **84** 144504

[211] Piña J C, de Souza Silva C C and Milošević M V 2012 Stability of fractional vortex states in a two-band mesoscopic superconductor *Phys. Rev.* B **86** 024512

[212] Zha G-Q, Wang Q and Zhou S-P 2013 Tunable periodic evolution and quantum phase transition in mesoscopic two-band superconducting loops *J. Appl. Phys.* **113** 213903

[213] Blatter G, Feigel'man M V, Geshkenbein V B, Larkin A I and Vinokur V M 1994 Vortices in high-temperature superconductors *Rev. Mod. Phys.* **66** 1125–388

[214] Gömöry F 1997 Characterization of high-temperature superconductors by AC susceptibility measurements *Supercond. Sci. Technol.* **10** 523–42

[215] Crisan A, Iyo A and Tanaka Y 2003 Vortex melting line and anisotropy of high-pressure-synthesized $TlBa_2Ca_2Cu_3O_{10-y}$ high-temperature superconductor from third-harmonic susceptibility studies *Appl. Phys. Lett.* **83** 506–8

[216] Stanley H E 1971 *Introduction to Phase Transitions and Critical Phenomena* (Oxford: Clarendon)

[217] Suzuki I S and Suzuki M 1988 Evidence of reentrant spin glass phase in graphite intercalation compound *Solid State Commun.* **106** 513–7

[218] Dekker C, Arts A F M, de Wijn H W, van Duyneveldt A J and Mydosh J A 1989 Activated dynamics in a two-dimensional Ising spin glass: $Rb_2Cu_{1-x}Co_xF_4$ *Phys. Rev.* B **40** 11243–51

[219] Goryo J, Soma S and Matsukawa H 2007 Deconfinement of vortices with continuously variable fractions of the unit flux quanta in two-gap superconductors *Eur. Phys. Lett.* **80** 17002

[220] Wilson K G 1974 Confinement of quarks *Phys. Rev.* D **10** 2445–559

[221] Loudon J C, Bowell C J, Zhigadlo N D, Karpinski J and Midgley P A 2013 Magnetic structure of individual flux vortices in superconducting MgB_2 derived using transmission electron microscopy *Phys. Rev.* B **87** 144515

[222] Goryo J, Saito T and Matsukawa H 2007 Vortex pinning in two-gap superconductors *J. Phys.: Conf. Ser.* **89** 012022

[223] Col A D, Geshkenbein V B and Blatter G 2005 Dissociation of vortex stacks into fractional-flux vortices *Phys. Rev. Lett.* **94** 097001

[224] Berezinskii V L 1971 Destruction of long-range order in one-dimensional and two-dimensional systems having a continuous symmetry group I. Classical systems *Sov. Phys. JETP* **32** 493–500

[225] Berezinskii V L 1972 Destruction of long-range order in one-dimensional and two-dimensional systems having a continuous symmetry group II. Quantum systems *Sov. Phys. JETP* **34** 610–6

[226] Kosterlitz J M and Thouless D J 1973 Ordering, metastability and phase transitions in two-dimensional systems *J. Phys. C: Solid State Phys.* **6** 1181–203

[227] Ruggiero S T, Barbee T W Jr and Beasley M R 1980 Superconductivity in quasi-two-dimensional layered composites *Phys. Rev. Lett.* **45** 1299–302

[228] Gammel P L, Schneemeyer L F, Wasczak J V and Bishop D J 1988 Evidence from mechanical measurements for flux-lattice melting in single-crystal $YBa_2Cu_3O_7$ and $Bi_{2.2}Sr_2Ca_{0.8}Cu_2O_8$ *Phys. Rev. Lett.* **61** 1666–9

[229] Houghton A, Pelcovits R A and Sudbø A 1989 Flux lattice melting in high-T_c superconductors *Phys. Rev.* B **40** 6763–70

[230] Benkraouda M and Clem J R 1996 Instability of a tilted vortex line in magnetically coupled layered superconductors *Phys. Rev.* B **53** 438

[231] Dodgson M J W, Koshelev A E, Geshkenbein V B and Blatter G 2000 Evaporation of the pancake-vortex lattice in weakly coupled layered superconductors *Phys. Rev. Lett.* **84** 2698–701

[232] Mints R G, Kogan V G and Clem J R 2000 Vortices in magnetically coupled superconducting layered systems *Phys. Rev.* B **61** 1623–9

[233] Fangohr H, Koshelev A E and Dodgson M J W 2003 Vortex matter in layered superconductors without Josephson coupling: numerical simulations within a mean-field approach *Phys. Rev.* B **67** 174508

[234] Crisan A, Iyo A, Tanaka Y, Matsuhata H, Shivagan D D, Shirage P M, Tokiwa K, Watanabe T, Button T W and Abell J S 2008 Magnetically coupled pancake vortex molecules in $HgBa_2Ca_{n-1}Cu_nO_y$ ($n \geqslant 6$) *Phys. Rev.* B **77** 144518

[235] Lounasmaa O V and Thuneberg E 1990 Vortices in rotating superfluid 3He *Proc. Natl. Acad. Sci. USA* **96** 7760–7

[236] Doi K and Natsume Y J 2001 Calculation of Bose–Einstein condensations and characteristic features of fluctuations for systems with ans without a vortex in two-component alkali atom gases *Phys. Soc. Japan* **70** 167–72

[237] Kasamatsu K, Tsubota M and Uead M 2004 Vortex molecules in coherently coupled two-component Bose–Einstein condensates *Phys. Rev. Lett.* **93** 250406

[238] Kasamatsu K, Tsubota M and Ueda M 2003 Vortex phase diagram in rotating two-component Bose–Einstein condensates *Phys. Rev. Lett.* **91** 150406

[239] Cipriani M and Nitta M 2013 Crossover between integer and fractional vortex lattices in coherently coupled two-component Bose–Einstein condensates *Phys. Rev. Lett.* **111** 170401

[240] Leslia L S, Hansen A, Wright K C, Deutcsh B M and Bigelow N P 2009 Creation and detection of skyrmions in a Bose–Einstein condensate *Phys. Rev. Lett.* **103** 250401

[241] Garaud J, Carlström J, Babaev E and Speight M 2013 Chiral *CP*2 skyrmions in three-band superconductors *Phys. Rev.* B **87** 014507

[242] Takahashi Y, Huang Z and Hu X 2014 *H–T* phase diagram of multi-component superconductors with frustrated inter-component couplings *J. Phys. Soc. Japan* **83** 034701

[243] Bardeen J and Stephen M J 1965 Theory of the motion of vortices in superconductors *Phys. Rev.* **140** A1197–207

[244] Lin S-Z and Bulaevskii L 2013 Dissociation transition of a composite lattice of magnetic vortices in the flux-flow regime of two-band superconductors *Phys. Rev. Lett.* **110** 087003

[245] Silaev M and Babaev E 2013 Unusual mechanism of vortex viscosity generated by mixed normal modes in superconductors with broken time reversal symmetry *Phys. Rev.* B **88** 220504(R)

[246] Silaev M A 2011 Stable fractional flux vortices and unconventional magnetic state in two-component superconductors *Phys. Rev.* B **83** 144519

[247] Lin S-Z and Reichhardt C 2013 Stabilizing fractional vortices in multiband superconductors with periodic pinning arrays *Phys. Rev.* B **87** 100508(R)

[248] Eigler D M and Schweizer E K 1990 Positioning single atoms with a scanning tunneling microscope *Nature* **344** 524–6

[249] Kasamatsu K, Takeuchi H, Tsubota M and Muneto N 2013 Wall-vortex composite solitons in two-component Bose–Einstein condensates *Phys. Rev.* A **88** 013620

[250] Tisza L 1938 Transport phenomena in Helium II *Nature* **141** 913–913

[251] Tisza L 1938 Sur lasupraconductibilitéthermique de l'hélium II liquide et la statistique de Bose–Einstein *C. R. Acad. Sci.* **207** 1035–7

[252] Tisza L 1938 La viscosité de l'hélium liquide et la statistique de Bose–Einstein *C. R. Acad. Sci.* **207** 1186–9

[253] London F 1938 On the Bose–Einstein condensation *Phys. Rev.* **54** 947–54

[254] Landau L 1949 On the theory of superfluidity *Phys. Rev.* **75** 884–5

[255] Donnelly R J 2009 The two-fluid theory and second sound in liquid helium *Phys. Today* **34** 34–9

[256] Donnelly R J 1995 The discovery of superfluidity *Phys. Today* **30** 30–6

[257] Tilley D R and Tilley J 1990 *Superfluidy and Superconductivity* 3rd edn (Bristol: Hilger)

[258] Sidorenkov L A, Tey M K, Grimm R, Y-Hau H, Pitaevskii L and Stringari S 2013 Second sound and the superfluid fraction in a Fermi gas with resonant interactions *Nature* **498** 78–81

[259] Gor'kov L P 1959 Microscopic derivation of the Ginzburg–Landau equations in the theory of superconductivity *Sov. Phys. JETP* **36** 1364–7

[260] Geilikman B T, Zaitsev R O and Kresin V Z 1967 Properties of superconductors having overlapping bands *Fiz. Tverd. Tela* **9** 821–9
Geilikman B T, Zaitsev R O and Kresin V Z 1967 *Sov. Phys.-Solid State* **9** 642–7

[261] Balian R and Werthamer N R 1963 Superconductivity with pairs in a relative p wave *Phys. Rev.* **131** 1553–64

[262] Strand J D, Bahr D J, Van Harlingen D J, Davis J P, Gannon W J and Halperin W P 2010 The transition between real and complex superconducting order parameter phases in UPt_3 *Science* **328** 1368–9

[263] Hess D W, Tokuyasu T A and Sauls J A 1989 Broken symmetry in an unconventional superconductor: a model for the double transition in UPt3 *J. Phys.: Condens. Matter* **1** 8135–45

[264] Schopohl N and Dolgov O V 1998 T dependence of the magnetic penetration depth in unconventional superconductors at low temperatures: can it be linear? *Phys. Rev. Lett.* **80** 4761–2

[265] Kuboki K and Sigrist M 1996 Proximity-induced time-reversal symmetry breaking at Josephson junctions between unconventional superconductors *J. Phys. Soc. Japan* **65** 361–4

[266] Matsunaga I M and Shiba H 1995 Coexistence of different symmetry order parameters near a surface in d-Wave superconductors *J. Phys. Soc. Japan* **64** 3384–96

[267] Matsunaga M and Shiba H 1995 Coexistence of different symmetry order parameters near a surface in d-Wave superconductors II *J. Phys. Soc. Japan* **64** 4867–81

[268] Matsunaga M and Shiba H 1996 Coexistence of different symmetry order parameters near a surface in d-Wave superconductors III *J. Phys. Soc. Japan* **65** 2194–203

[269] Goryo J 2003 Phenomenology for multiple phases in the heavy-fermion skutterudite superconductor $PrOs_4Sb_{12}$ *Phys. Rev.* B **67** 184511

[270] Lee W-C, Zhang S-C and Wu C 2009 Paring state with a time-reversal symmetry breaking in FeAs-Based superconductors *Phys. Rev. Lett.* **102** 217002

[271] Iniotakis C, Fujimoto S and Sigrist M J 2008 Fractional flux quanta at intrinsic metallic interfaces of noncentrosymmetric superconductors *Phys. Soc. Japan* **77** 083701

[272] Lin S-Z 2012 Josephson effect between a two-band superconductor with s++ or s± pairing symmetry *Phys. Rev.* B **86** 014510

[273] Kondo J 2002 Theory of multiband superconductivity *J. Phys. Soc. Japan* **71** 1353–9

[274] Konsin P, Kristoffel N and Örd T 1988 The interband interaction as a possible cause of high-temperature superconductivity *Phys. Lett.* A **129** 339–42

[275] Chakraverty B K 1993 Superconductive solutions for a two-band Hamiltonian *Phys. Rev.* B **48** 4047–53

[276] Yamaji K and Shimoi Y 1994 Superconducting transition of the two-chain Hubbard model indicated by diagonalization calculations *Physica* C **222** 349–60

[277] Yamaji K, Shimoi Y and Yanagisawa T 1994 Superconductivity indications of the two-chain Hubbard model due to the two-band effect *Physica* C **235–240** 2221–2

[278] Combescot R and Leyronas X 1995 Coupling between planes and chains in $YBa_2Cu_3O_7$: a possible solution for the order parameter controversy *Phys. Rev. Lett.* **75** 3732–5

[279] Shirage P M, Kihou K, Miyazawa K, Lee C-H, Kito H, Eisaki H, Yanagisawa T, Tanaka Y and Iyo A 2009 Inverse iron isotope effect on the transition temperature of the (Ba, K)Fe_2As_2 superconductor *Phys. Rev. Lett.* **103** 257003

[280] Fröhlich H 1950 Theory of the superconducting state. I. The ground state at the absolute zero of temperature *Phys. Rev.* **79** 845–56

[281] Maxwell E 1950 Isotope effect in the superconductivity of mercury *Phys. Rev.* **78** 477

[282] Reynolds C A, Serin B, Wright W H and Nesbitt L B 1950 Superconductivity of isotopes of mercury *Phys. Rev.* **78** 487

[283] Kuroki K, Onari S, Arita R, Usui H, Tanaka Y, Kontani H and Aoki H 2008 Unconventional pairing originating from the disconnected fermi surfaces of superconducting $LaFeAsO_{1-x}F_x$ *Phys. Rev. Lett.* **101** 087004

[284] Mazin I I, Singh D J, Johannes M D and Du M H 2008 Unconventional superconductivity with a sign reversal in the order parameter of $LaFeAsO_{1-x}F_x$ *Phys. Rev. Lett.* **101** 057003

[285] Golubov A A and Mazin I I 1995 Sign reversal of the order parameter in s wave superconductors *Physica* C **243** 153–9

[286] Onari S, Arita R, Kuroki K and Aoki H 2003 Superconductivity in repulsive electron systems with three-dimensional disconnected Fermi surfaces *Phys. Rev.* B **68** 024525

[287] Yanagisawa T, Odagiri K, Hase I, Yamaji K, Shirage P M, Tanaka Y, Iyo A and Eisaki H 2009 Isotope effect in multi-band and multi-channel attractive systems and inverse isotope effect in iron-based superconductors *J. Phys. Soc. Japan* **78** 094718

[288] Shirage P M, Miyazawa K, Kihou K, Kito H, Yoshida Y, Tanaka Y, Eisaki H and Iyo A 2010 Absence of an appreciable iron isotope effect on the transition temperature of the optimally doped $SmFeAsO_{1-y}$ superconductor *Phys. Rev. Lett.* **105** 037004

[289] Tsuge Y, Iyo A, Tanaka Y, Eisaki H and Nishio T 2012 Inverse iron isotope effect in $FeSe_{0.35}Te_{0.65}$ *Physica Proc.* **36** 731–4

[290] Choi H-Y, Yun J H, Bang Y and Lee H C 2009 Model for the inverse isotope effect of FeAs-based superconductors in the π-phase-shifted pairing state *Phys. Rev.* B **80** 052505

[291] Tanaka Y, Shirage P M and Iyo A 2010 Disappearance of meissner effect and specific heat jump in a multiband superconductor, $Ba_{0.2}K_{0.8}Fe_2As_2$ *J. Supercond. Nov. Magn.* **23** 253–6

[292] Storey K J G, Loram J W, Cooper J R, Bukowski Z and Karpinski J 2013 Electronic specific heat of $Ba_{1-x}K_xFe_2As_2$ from 2 to 380 *Phys. Rev.* B **88** 144502

[293] Tanaka Y, Shirage P M and Iyo A 2010 Time-reversal symmetry-breaking in two-band superconductors *Physica* C **470** 2023–6

[294] Maiti S and Chubukov A V 2013 s+ is state with broken time-reversal symmetry in Fe-based superconductors *Phys. Rev.* B **87** 144511

[295] Stanev V and Koshelev A E 2014 Complex state induced by impurities in multiband superconductors *Phys. Rev.* B **89** 100505(R)

[296] Garaud J and Babaev E 2014 Domain walls and their experimental signatures in s+ is superconductors *Phys. Rev. Lett.* **112** 017003

[297] Lee T D 1973 A theory of spontaneous T Violation *Phys. Rev.* D **8** 1226–39

[298] Tanaka Y and Yanagisawa T 2010 Chiral state in three-gap superconductors *Solid State Commun.* **150** 1980–2

[299] Wilson B J and Das M P 2013 Time-reversal-symmetry-broken state in the BCS formalism for a multi-band superconductor *J. Phys.: Condens. Matter* **25** 425702

[300] Scalapino D J, Schrieffer J R and Wilkins J W 1966 Strong-coupling superconductivity. I *Phys. Rev.* **148** 263–79

[301] Dias R G and Marques A M 2011 Frustrated multiband superconductivity *Supercond. Sci. Technol.* **24** 085009

[302] Orlova N V, Shanenko A A, Milošević M V, Peeters F M, Vagov A V and Axt V M 2013 Ginzburg–Landau theory for multiband superconductors: microscopic derivation *Phys. Rev.* B **87** 134510

[303] Nambu Y and Jona-Lasinio G 1961 Dynamical model of elementary particles based on an analogy with superconductivity. I *Phys. Rev.* **122** 345–58

[304] Higgs P W 1964 Broken symmetries and the masses of gauge bosons *Phys. Rev. Lett.* **13** 508–9

[305] Ota Y, Machida M, Koyama T and Aoki H 2011 Collective modes in multiband superfluids and superconductors: multiple dynamical classes *Phys. Rev.* B **83** 060507

[306] Anishchanka A, Volkov A F and Efetov K B 2007 Collective modes in two-band superconductors in the dirty limit *Phys. Rev.* B **76** 104504

[307] Tisza L 1949 On the theory of superfluidity *Phys. Rev.* **75** 885–6

[308] Peshkov V P and Stryukov V B 1962 Which is responsible for the destruction of superfluidity v_s or v_s-v_n *Sov. Phys. JETP* **14** 1031–4
Peshkov V P and Stryukov V B 1961 *J. Exp. Theor. Phys.* **41** 1443–8

[309] Peshkov V P, Daunt J G and Harrison J P 1981 In memoriam *J. Low Temp. Phys.* **42** i

[310] Atkins K R 1959 *Liquid Helium* (London: Cambridge University Press)

[311] Carlson R V and Goldman A M 1976 Dynamics of the order parameter of superconducting aluminum films *J. Low Temp. Phys.* **25** 67–97

[312] Tanaka Y, Yanagisawa T and Nishio T 2013 Unlocking interband phase difference in multiband superconductors *Physica* C **485** 64–70

[313] Tanaka Y, Iyo A, Itoh S, Tokiwa K, Nishio T and Yanagisawa T 2014 Experimental observation of a possible first-order phase transition below the superconducting transition temperature in the multilayer cuprate superconductor $HgBa_2Ca_4Cu_5O_y$ *J. Phys. Soc. Japan* **83** 074705

[314] Bojesen T A, Babaev E and Sudbø A 2013 Time reversal symmetry breakdown in normal and superconducting states in frustrated three-band systems *Phys. Rev.* B **88** 220511(R)

[315] Regal C 2006 Experimental realization of BCS-BEC crossover physics *PhD Thesis* University of Colorado

[316] Nozières P and Schmitt S-R 1985 Bose condensation in an attractive fermion gas: from weak to strong coupling superconductivity *J. Low Temp. Phys.* **59** 195–211

[317] Leggett A J 1980 Cooper pairing in spin-polarized fermi systems *J. Phys. (Paris)* **41** C7–10

[318] Eagles D M 1969 Possible pairing without superconductivity at low carrier concentrations in bulk and thin-film superconducting semiconductors *Phys. Rev.* **186** 456–63

[319] Leggett A J 1980 Diatomic molecules and cooper pairs *Mod. Trends Theor. Condens. Matter* **115** 13–27

[320] Schaforth M R 1958 Remarks on the meissner effect *Phys. Rev.* **111** 72–4

[321] Schafroth M R 1955 Connection between suyerfluidity and suyerconductivity *Phys. Rev.* **100** 502–5

[322] Sickinger H, Lipman A, Weides M, Mints R G, Kohlstedt H, Koelle D, Kleiner R and Goldobin E 2012 Experimental evidence of a φ Josephson junction *Phys. Rev. Lett.* **109** 107002

[323] Ryazanov V V, Oboznov V A, Rusanov A, Yu, Veretennikov A V, Golubov A A and Aarts J 2001 Coupling of two superconductors through a ferromagnet: evidence for a π junction *Phys. Rev. Lett.* **86** 2427–30

[324] Huang Z and Hu X 2014 Josephson effects in three-band superconductors with broken time-reversal symmetry *Appl. Phys. Lett.* **104** 162602

[325] Schmidt S, Doring S, Schmidl F, Grosse V, Seidel P, Iida K, Kurth F, Haindl S, Mönch I and Holzapfel B 2010 $BaFe_{1.8}Co_{0.2}As_2$ thin film hybrid Josephson junctions *Appl. Phys. Lett.* **97** 172504

[326] Doring S, Schmidt S, Schmidl F, Tympel V, Haindl S, Kurth F, Iida K, Monch I, Holzapfel B and Seidel P 2012 Edge-type Josephson junctions with Co-doped Ba-122 thin films *Supercond. Sci. Technol.* **25** 084020

[327] Raghu S, Kivelson S A and Scalapino D J 2010 Superconductivity in the repulsive Hubbard model: an asymptotically exact weak-coupling solution *Phys. Rev.* B **81** 224505

[328] Zhang S C 1997 A unified theory based on SO(5) symmetry of superconductivity and sntiferromagnetism *Science* **275** 1089–96

[329] Baskaran G 2009 Five-fold way to new high T_c superconductors *Current Trends in Science—Platinum Jubilee Special* ed N Mukunda (Bangalore: Indian Academy of Sciences) Section Physics pp 279–309

[330] Baskaran G and Anderson P W 1988 Gauge theory of high-temperature superconductors and strongly correlated Fermi systems *Phys. Rev.* B **37** 580–3

[331] Florens S and Georges A 2004 Slave-rotor mean-field theories of strongly correlated systems and the Mott transitionin finite dimensions *Phys. Rev.* B **70** 035114

[332] Pathak S, Shenoy V B and Baskaran G 2010 Possible high-temperature superconducting state with a d+id pairing symmetry in doped graphene *Phys. Rev.* B **81** 085431

[333] Tanaka Y 2014 Superconducting frustration bit *Physica* C **505** 55–64